Department of Environment Systems

Graduate School of Frontier Sciences

The University of Tokyo

2023

Master's Thesis

Preparation of Silver Nanoparticles via Continuous Hydrothermal Synthesis Method

（連続式水熱合成法による銀ナノ粒子の調製）

20th, July 2023

Supervisor: Associate Professor Akizuki Makoto

LI Yanchen

Catalogue

Chapter 1 Introduction

1.1 Nanoparticles

Nanoparticles refer to particles that have dimensions in the range of 1 to 100 nanometers. They can be composed of various materials, including metals, ceramics, polymers, and biological substances, and these tiny particles possess unique properties and behaviors compared to their bulk counterparts due to their small size and high surface-to-volume ratio. Compared with general inorganic materials, inorganic nanomaterials have different optical, electrical, magnetic, thermal, mechanical and mechanical properties than ordinary materials due to their nanometer size, which can exhibit surface effect, small size effect, macroscopic quantum tunneling effect and quantum confinement effect, and therefore have broad application prospects in optical materials, electronic materials, magnetic materials, thermal conductive materials, high density materials, etc. Therefore, the preparation of nanoparticle materials has become a key area of chemical engineering.

Until now, nanoparticles have gained significant attention in various fields, including medicine, electronics, energy, and environmental science, due to their wide range of applications and potential benefits.

1.2 Silver Nanoparticles and Synthesis Methods

1.2.1 Application of Silver Nanoparticles

Silver (Ag) is a noble metal with abundant reserves and good physical properties. Silver has high ductility, electrical and thermal conductivity, and has a wide range of applications in electronic and electrical appliances, photosensitive materials, chemical materials and other fields. With the continuous development of nanotechnology, the good electrical conductivity, thermal conductivity, antibacterial properties, optical properties and other special properties of nano-silver have been widely developed and applied.

Silver nanoparticles have distinct physical, chemical and biological properties. It is widely used in medicine, biosensors, catalyst, electronics, and environmental remediation. One of the most significant properties of silver nanoparticles is their antimicrobial activity. The small size of these particles allows them to penetrate bacterial and fungal cells, leading to their destruction. As a result, silver nanoparticles are used in a variety of medical and healthcare products, such as wound dressings,

surgical instruments, and antibacterial coatings for medical equipment [1].

Silver nanoparticles are also used in electronics and energy applications due to their electrical conductivity. They are used in conductive inks, sensors, and catalysts for fuel cells. Additionally, silver nanoparticles are used in water treatment processes to remove contaminants such as heavy metals and organic compounds [2].

1.2.2 Synthesis Methods of Silver nanoparticles

Nanoparticles can be produced via different techniques, which can be grouped into two main categories: bottom-up and top-down methods [3]. That means the pulverization of raw materials into particles, including Sol-gel, spinning, chemical vapor deposition (CVD), Physical Vapor Deposition (PVD), pyrolysis and biosynthesis, and the precipitation of particles from precursors such as ions and molecules, including Mechanical milling, nanolithography, laser ablation, sputtering and thermal decomposition (Figure 1.1).

Specifically for nano-silver, the preparation of AgNPs (silver nanoparticles) can be achieved through different techniques, which are typically classified into three categories: chemical, physical, and biological methods [4].

It is worth mentioning that the chemical methods have been identified as an efficient, convenient, and easily manageable approach compared to other methods. Chemical reduction is commonly used and high productivity with minimal cost can be achieved using this approach. In chemical reduction, silver ions are reduced to form silver nanoparticles using a reducing agent such as sodium borohydride [5], citrate [6], or ascorbic acid. The reaction can be carried out in solution or on a solid support, and the size and shape of the resulting nanoparticles can be controlled by adjusting the reaction conditions such as temperature, pH, and concentration of reactants. However, it is important to note that the chemical reduction method may involve the use of hazardous chemicals, and the chemical waste solution are harmful to humans.

By physical methods, such as electric energy, light energy, microwave plasma, and vacuum evaporation-condensation [1], there is no solvent contamination in the process, and the distribution of synthesized nanoparticles is homogeneous. However, the physical synthesis of AgNPs also has some disadvantages including high energy consumption, low production rate and complicated operation.

Biosynthesis of AgNPs using reducing agents like biological microorganism, polysaccharides, plants extracts, bacteria or fungus is in line with the concept of green chemistry [7], which do not use pollutants from the source through scientific research and development. In most cases, silver nanoparticle is one of the recognized particles with biotic characteristics. In short, biological synthesis method of nano-silver is a cost effective and an environmentally stable approach but it is difficult to produce

nanoparticles at a large scale.
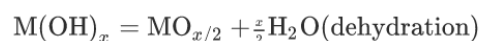
1.3 Supercritical Hydrothermal Synthesis

1.3.1 Properties of High-temperature and High-pressure Water

The physical properties of high-temperature, high-pressure water, such as density, dielectric constant, and ionic product, change drastically and with temperature manipulation, and the temperature dependence of water properties at 25 MPa is shown in Figure 1.2.

Water above the critical point (374 °C, 22.1 MPa) is referred to supercritical water, its density is lower than that of liquid water but is much higher than that of steam [9]. The density of water decreases slowly with increasing temperature and rapidly near the critical point, such density changes also have a significant effect on the temperature dependence of the dielectric constant and ion product. The dielectric constant of water decreases with increasing temperature, and above the critical point, it takes a low value comparable to that of non-polar solvents. Such a drastic change in permittivity is closely related to the stability of metal ions and, consequently, to the solubility and the formation rate of metal oxides. In short, lower dielectric constant and solubility of ions can lead to hydrothermal reactions with high reaction rates.

1.3.2 Synthesis of Nanoparticles via High-temperature and High-pressure Water

The hydrothermal synthesis method is one of the methods for synthesizing metal oxides using high-temperature and high-pressure water. Metal ions react with water at high temperature and pressure to form hydroxides, which are then dehydrated to produce metal oxide precipitates. Up to now, the synthesis of wide variety of metal oxide NPs by supercritical hydrothermal method has been achieved [10]. In this method, metal ions are hydrolyzed in supercritical water to form hydroxides, which are then dehydrated to metal oxides. The dissolution equilibrium of metal salts shifts toward the formation of hydroxides and then oxides as the temperature is increased.

$$M(NO_3)_x + xH_2O = M(OH)_x + xHNO_3 \, (\text{hydrolysis})$$

$$M(OH)_x = MO_{x/2} + \tfrac{x}{2}H_2O \, (\text{dehydration})$$

When the concentration of the oxide exceeds the saturation solubility, precipitation occurs. Generally, precipitation does not occur immediately after the saturated solubility is exceeded, but only after supersaturation has reached a certain degree of supersaturation. This precipitation process is nucleation. When nucleation occurs, the oxide concentration drops rapidly. (Figure 1.3) The greater the degree of

supersaturation, the greater the nucleation rate. Thus, when the degree of supersaturation is increased, it leads to the formation of a larger number of smaller nuclei. While the supersaturation will be used to grow the microcrystals after nucleation, the more small-nuclei produced, the smaller the final particle size produced. And at the supercritical region, fast reaction rate and low solubility can lead to an extremely high nucleation rate, which allows the formation of nano-sized particles.

The utilization of water as a solvent in this method is not only cost-effective, but also highly eco-friendly and non-toxic. In addition, the pressurization allows the use of high temperatures, which results in oxide particles with good crystallinity. And high-temperature, high-pressure water has low kinematic viscosity and a large diffusion coefficient, making it easy to provide a highly uniform reaction field. Furthermore, the reaction time for synthesizing NPs is also remarkably shorter compared to traditional wet processes for fine NPs synthesis.

1.3.3 Continuous Supercritical Hydrothermal Synthesis

The basic process of continuous supercritical hydrothermal synthesis is: One material is mixed with supercritical water preheated to the supercritical state and then meets and reacts with another material in the reactor. The resulting hydroxide is dehydrated and precipitates out of solution as nanomaterials driven by very high supersaturation and finally collected in a collector. The key step of the continuous supercritical hydrothermal synthesis process is the rapid mixing of supercritical water with low-temperature metal salt solutions (precursors) in a specific mixer to achieve rapid temperature rise and rapid reaction using the large specific heat capacity of supercritical water.

Compared to the batch system, continuous supercritical hydrothermal synthesis (the flow system) has the following advantages:

(1) High production efficiency. Batch type hydrothermal synthesis units are tedious in terms of dosing, heating, and product recovery, resulting in low yields and high labor costs. Continuous supercritical hydrothermal synthesis can achieve continuous production and collection of target products, so the efficiency is greatly improved.

(2) Particle size is easier to control. Batch type hydrothermal synthesis has a slow heating rate and the overgrowth of particles is prone to appear during the reaction. Continuous supercritical hydrothermal synthesis can achieve rapid heating and cooling of the reaction fluid, resulting in finer nanoparticles with more controllable particle size.

(3) Easy to realize the preparation of functionalized materials. Batch type hydrothermal synthesis can only mix the materials and heat them at the same time, while continuous supercritical hydrothermal synthesis is easy to expand to multi-stage feeding, which can realize the preparation of functionalized nanoparticles such as

bimetals.

1.4 Stabilizing Agents

The high surface area to volume ratio of the NPs results in high reactivity, which leads to particle aggregation and settling, thus the protection by a capping agent that provides colloidal stability through electrostatic or steric repulsion is needed.

Noble metal particles in high ionic strengths or organic-phase suspensions are usually stabilized by capping agents, including surfactants [12], polymers [13], self-assembled monolayers [14] or stabilizing ligands [15]. Along with the assistance of a stabilizing agent, various factors can be influenced, including the long-term stability of metal nanoparticles, the ability to control the distribution of particle sizes and alter the shape of nanocrystals [16], and the aggregation of the metal clusters [18].

The conventional method for synthesizing Ag nanoparticles involves reducing Ag^+ ions in a liquid medium, such as water or organic solvents, typically with the aid of a stabilizing agent. It is worth mentioning that the large positive reduction potential of Ag makes its nanoparticles less susceptible to oxidation, resulting in quite stable aqueous or alcoholic suspensions without the need of antioxidants. On the other hand, when the synthesis of Ag particles is carried out in the presence of a capping agent, different shapes may be formed due to the different affinities of the capping agent towards the exposed crystal faces [17].

Due to unoccupied orbitals present on the Ag nanoparticle surface, the nucleophiles can donate the electrons, thereby weakly complexing the Ag particles. This particular mechanism can be used to stabilize colloidal Ag nanoparticles.

Sodium dodecyl sulfate (SDS), Tween 80 and Polyvinylpyrrolidone (PVP) exhibit superior stabilization of the silver NPs dispersions against the process of aggregation [19]. However, the first two stabilizers, although more effective, cannot withstand high temperatures and therefore cannot be utilized in supercritical hydrothermal synthesis.

As one of the best polymeric stabilizers for Ag nanoparticles in aqueous solutions, Polyvinylpyrrolidone (PVP) $(C_6H_9NO)_n$ is an inert, non-toxic, temperature-resistant, pH-stable, biodegradable polymer, its structure is shown in Figure 1.4. In larger particles (>50 nm), steric effects dominate stabilizing; For particles <50 nm, the main factor influencing interaction between PVP and Ag is the coordination of N, and O to Ag. It coordinates to Ag particles via the N or O atoms, and generates a covering layer on the particle surface which inhibits growth and agglomeration. Due to the higher capacity of N to donate electrons, the interaction between N and Ag^+ is more important than that between O and Ag. And as a stabilizer, it can enhance the antibacterial activity of the silver NPs in a significant extent, this is because the polymer can stabilize the

NPs against aggregation. The non-aggregated NPs are able to interact strongly with the cell wall because of their high surface energy and mobility that are not lowered by the formation of spacious aggregates. Therefore, Polyvinylpyrrolidone (PVP) can not only play a role in the synthesis, but also keep the excellent properties of the product.

1.5 Production of silver nanoparticles in supercritical water

1.5.1 Preparation of Metal Nanoparticles in SC-water

The effective production and environmentally benign process of high-quality NPs are encouraged to be developed in nanotechnology.

Until now, the synthesis of a variety of metal oxide NPs via supercritical hydrothermal method has been developed. Water, one of the most environmentally friendly, non-toxic, cheap solvents, is used as the solvent in this method. And in addition, by SHS, the reaction time required to synthesize NPs is extremely shorter than the any other conventional wet chemical synthesis process of metal oxide NPs. It would be compelling development on hydrothermal synthesis method of NPs if the applicability of this method and its reaction system spread to the metal NPs production.

Because water can catalyze oxidation of metals and water itself can oxidize metals, it is not so easy to apply supercritical hydrothermal synthesis to the production of metal NPs. At present, hydrogen is generally used as the reducing agent when preparing metal nanoparticles. Arita et al. studied the synthesis of metal Ni, Pd, Fe, Cu, and Ag particles with batch methods, and they used formic acid (HCOOH) additives that decompose to hydrogen at reaction conditions, as reducing agent [20]. The rationale for designing the experiment in this way is as follows:

I. Almost all the formic acids decomposed in SC-water condition are converted to H_2 and CO_2.

II. Formic acid is in the liquid state, it is more convenient to load than H_2 gas.

III. The equilibrium of WGSR in SC-water is sided to H_2 generation because of large excess amount of water molecules.

Although in their experiments, no surface modifier was employed so that the metal NPs obtained were all agglomerated and aggregated (Even from the TEM image, for silver, only nano-dendrites are formed instead of nanoparticles), the results confirmed that zero-valent silver and copper could be synthesized with the supercritical hydrothermal synthesis method.

Shigeki Kubota et al. referred to Arita's research, adopted formic acid as a reducing agent to synthesize Copper nanoparticles by continuous supercritical hydrothermal method, with copper formate tetrahydrate as the precursor of Cu [21]. In their

experiments the zero-valent Cu nanoparticles were formed, which had particle size of 17-42 nm, were spherical in shape and contained no oxide contaminants.

Also using formic acid as a reducing agent, Gimyeong Seong et al. successfully synthesized highly crystalline cobalt nanoparticles with low surface oxidation via supercritical hydrothermal process in the temperature range of 340~420 °C [31]. In their experiments, pure Co was only obtained when the molar ration of formic acid to cobalt salt was above a certain value.

1.5.2 The Silver Nanoparticles Prepared in SC-water

In the past, some studies on the synthesis of silver nanoparticles using supercritical water have been reported. Li and Zhang used Ag microparticles as precursors, prepared Ag nanoparticles in supercritical water [22]. Their experiment results revealed that Ag microparticles with the sizes < 1μm were successfully destroyed and formed Ag nanoparticles via the destructive effect of SC-water. It has also been reported that in SC-water, Ag aggregates could be broken up and the resulting Ag nanoparticles could be organized into nanowires and triangle nano-banners [23]. In the initial stage of their experiment, the Ag aggregates were broken down into nanoparticles, which exhibited a size distribution ranging from 2 to 20 nm. And there is a limited amount of research reports available regarding the use of hydrothermal synthesis to prepare silver nanoparticles directly from metal salt precursors.

Using glycerol as the reducing agent, Minsoo Kim et al. reduced silver, copper and nickel nitrates into zero-valent metal nanoparticles at 400 °C and 300 bar by batch-type supercritical hydrothermal synthesis method [32]. However, the metal nanoparticles obtained in this series of experiments have large particle sizes, ranging from 2000 to 5000 nm for silver nanoparticles and 200 to 2000 nm for copper nanoparticles.

1.5.3 Preparation of AgNPs by Continuous Supercritical Hydrothermal Synthesis

Junichi Otsu et al. used a batch-type reactor (30 MPa, 400°C) with supercritical water to prepare silver oxide particles on the surface of alumina but finally obtain silver particles. They speculate the reason for the formation of metal silver is that silver is thermodynamically more stable than metal oxide at high-temperature conditions [24]. And according to a study of Gabriele Aksomaityte et al., using silver acetate as the precursor, they successfully achieved the production of silver nanoparticles via continuous supercritical hydrothermal synthesis, it has been confirmed that metal silver was obtained under supercritical conditions (380°C to 430°C) without reducing agents [25]. In their experiments, the silver nanoparticles with the average particle size of 30–40 nm was prepared at 415 °C, and raising the temperature from 380 °C to 430 °C within the reaction zone resulted in a reduction in the particle size.

It is hypothesized that, similar to the formation of metal oxide nanoparticles in general, silver oxide is formed from a silver salt solution in supercritical water before it is converted to silver nanoparticles.

The Possible mechanisms for Ag:

$$AgAc + \frac{1}{2}H_2O = \frac{1}{2}Ag_2O + \frac{1}{2}HAc$$
$$Ag_2O = 2Ag + \frac{1}{2}O_2$$
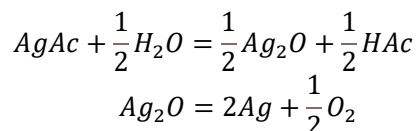
Unlike the preparation of other metal nanoparticles, the reaction is completed under supercritical conditions without the involvement of a reducing agent. If this hypothesized mechanism is correct, the reducing agent may be needed at lower temperatures under subcritical conditions.

1.5.4 Conversion of Silver oxide to Silver

Lewis decomposes silver oxide in 1atm oxygen at 320~350°C, and the process is very slow. They believe that the decomposition rate is related to the preparation method of the sample. Pavlyuchenko and Gurevich used Ag_2O prepared at a lower temperature and found that the decomposition temperature in vacuum was 118-220 °C. In Garner's article, Ag_2O prepared by precipitation at 100°C is used, and then aged in a high-pressure oxygen atmosphere at 200~300°C. At 185 °C, no gas was generated within two hours [26]. At a pressure of 50 mmHg and a heating rate of 200 °C/h, Ag_2O sample is produced by the decomposition of silver carbonate. The decomposition of Ag_2O occurs at 354°C [27]. In a nitrogen atmosphere, at a heating rate of 2°C/min, Ag_2O starts to decompose at 330°C, the decomposition rate is the highest at 440°C, and the decomposition is completed at 500°C [28].

In the 21st century, according to Lange's Handbook of Chemistry, Ag_2O decomposes from 200°C [29]. And in a study using XRD, infrared and Raman spectroscopy, Ag_2O is stable up to 350 °C. At 400°C, Ag_2O is completely decomposed into Ag and O_2 [30].

The decomposition temperatures of silver oxide reported in these literatures are different. The possible reason is that the thermal decomposition of silver oxide is a reversible reaction and also an autocatalytic reaction, and the factors such as the preparation method of the silver oxide, the state of the silver oxide, and the concentration of oxygen will affect the experimental results. Judging from these literatures, in general, the obvious decomposition of silver oxide is above 300 °C or even 350 °C and there may be a very small amount of decomposition in the range of 100~200 °C.

Therefore, assuming that the conversion of silver oxide to silver can be completed or silver is more inclined to exist than silver oxide in supercritical water (above 374°C),

the preparation of nano-silver under corresponding conditions does not require the use of reducing agents.

1.6 Research Objective

Considering that the temperature for the conversion of Ag_2O to Ag are different, which can be below the critical point, it's possible that nano-silver can be formulated even under subcritical conditions (temperature below supercritical conditions) without requiring the use of reducing agents.

Therefore, this study aims to achieve the one-step preparation of Ag nanoparticles by CHS under subcritical conditions and explore the preparation conditions (including precursor type, concentration, residence time and so on) to realize size-controllable synthesis.
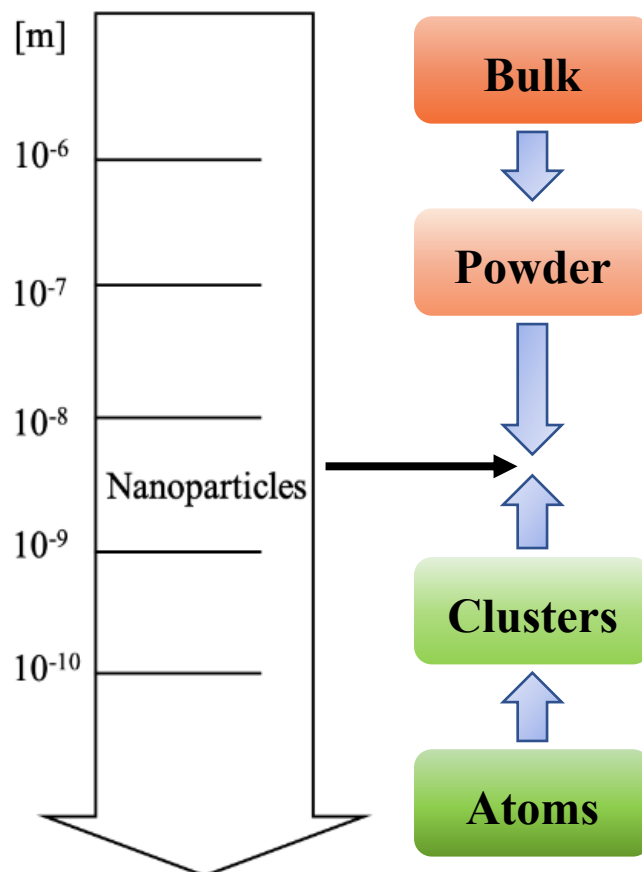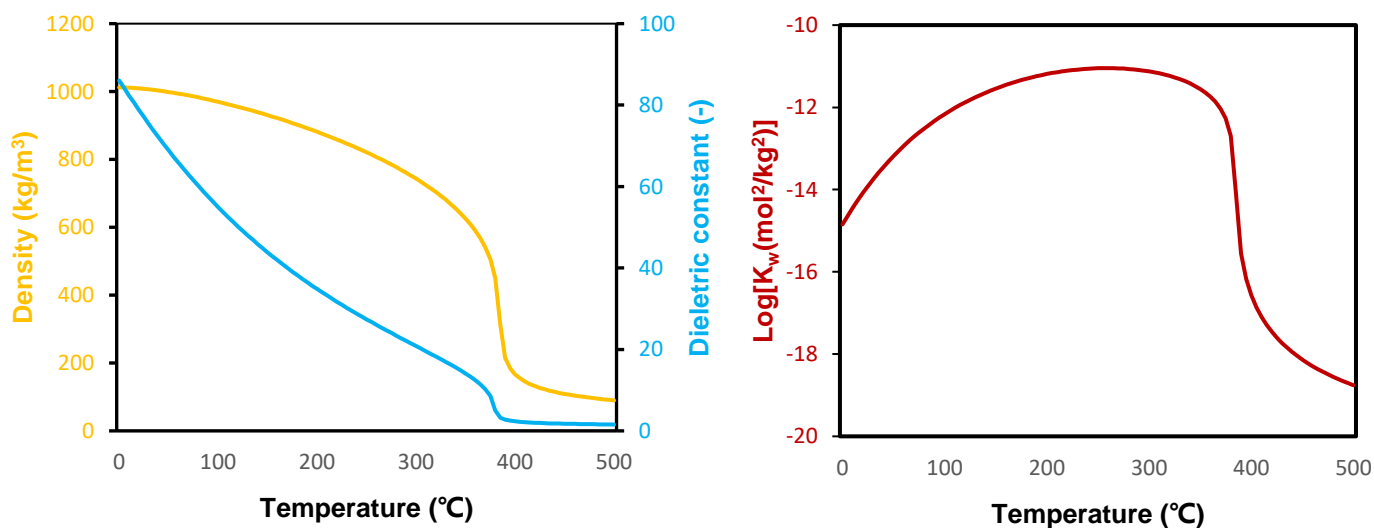
Figure 1.1 Particles synthesis methods
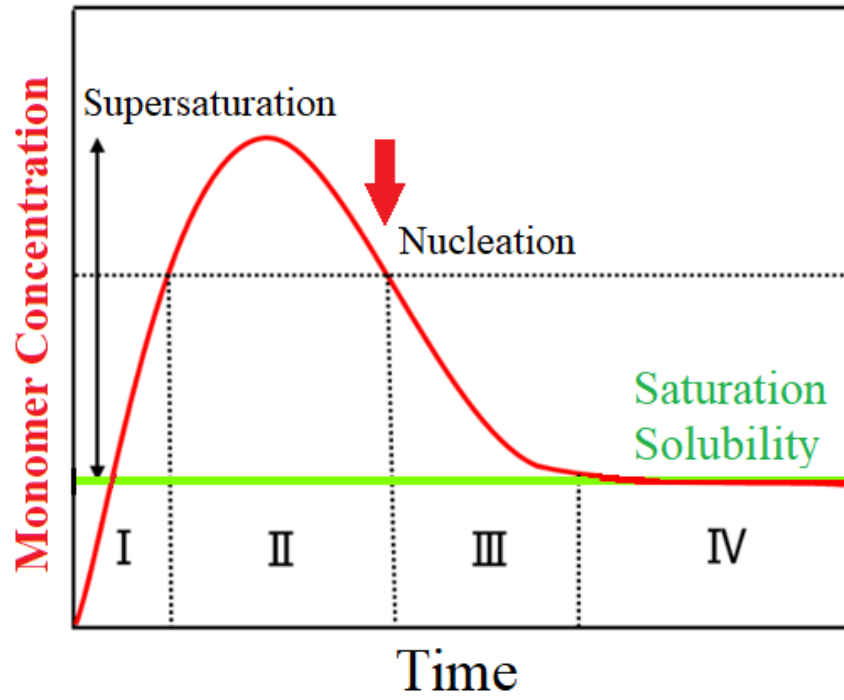

Figure 1.2 Properties of water at 25 MPa [8-9]

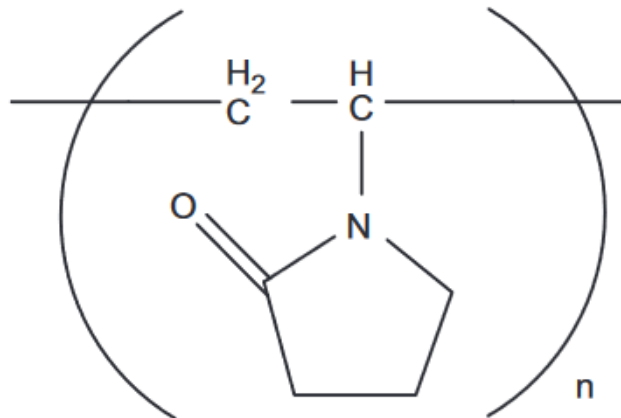**Figure 1.3 Relationship between nucleation and supersaturation [11]**

Figure 1.4 Structure of Polyvinylpyrrolidone (C6H9NO)n

Chapter 2 Methodology

2.1 Materials

The following reagents were used in the experiments.

- Distilled water, purified by AQUARIUS (made by RFD240HA, ADVANTEC)
- CH_3COOAg Wako Pure Chemicals
- $AgNO_3$ Wako Pure Chemicals
- $(C_6H_9NO)n$ (Polyvinylpyrrolidone 40)   Wako Pure Chemicals
- HNO_3 Wako Pure Chemicals
- NaOH   Wako Pure Chemicals
- Ethanol (99.5%)   Wako Pure Chemicals

2.2 Apparatus and Procedure

As shown in Figure 2.1, the continuous hydrothermal synthesis experiments were conducted using the flow-type reaction apparatus with a newly designed reactor, which is constructed with reference to the Nozzle reactor designed by Edward Lester et al [31]. The reactor consists of outer diameter 1/4 inch., inner diameter 3.75 mm and length 160 mm, and the water tubes' type is 1/16 inch. Since the synthesis of metal nanoparticles using a continuous system is prone to clogging of the pipeline, this reactor is designed to prevent clogging and allow the reaction to proceed smoothly.

Silver salt solution was used as a raw material, mixed with hot distilled water heated in a sand bath, started reaction in the reactor and ended in the cooler. The distilled water is first pumped into the sand bath furnace to complete the heating, and then into the slender pipe inside the reactor, where it is mixed under high temperature and pressure with the silver salt solution that is pumped into the reactor at the same time. The pressure was adjusting by the back pressure valve (BP66-112865, Go Inc) setting at the outlet. The experiments in this study were conducted at a pressure of 25 MPa.

The nanoparticle suspension products were collected in jars. And then the suspension was subjected to the pressure filtration with nitrogen (about 0.2 MPa) through a nitrocellulose filter (Millipore, pore size: 25 nm, VSWP14250). After filtration, the product on the filter was rinsed into a beaker with distilled water, and then was dried by a vacuum dryer (Yamato, ADP-31) to collect the solid particles. One thing to note is that for silver nanoparticles, if sending the filter to vacuum dryer directly, it will form a layer of extremely strong silver mirror which cannot be gotten off.

Two experiments were conducted in a batch reactor, using silver oxide powder as raw material, mixed with saturated water heated in a sand bath. When the set residence time was up, the reactor was placed in water for rapid cooling and the product was removed.

2.3 Characterization

TEM and XRD were used to observe the synthesized particles. ICP emission spectrometry was used to measure the concentration of silver ions in solution to calculate the conversion rates.

2.3.1 XRD

For the produced nanoparticles, the substance composition was identified and the crystallite size was evaluated by X-ray diffraction (Rigaku, SmartLab). The basic measurement conditions are scanning speed: 4 degree/min, slit: 2/3, running range: 10-90 degrees, step width: 0.02 degree, and goniometer radius: 300 mm. The X-ray source was a CuKα ray (λ = 1.5418 Å), and the measurements were performed by a Bragg-Brentano diffraction system. The crystallite size was calculated from the obtained XRD patterns. The Scherrer equation is expressed as follows.

$$\tau = \frac{K\lambda}{\beta cos\theta}$$

τ: Crystal size
K: Dimensionless shape factor
λ: X-ray wavelength
β: Line broadening at half the maximum intensity
θ: Bragg angle

2.3.2 TEM

Transmission Electron Microscopy (TEM) is a popular technique used to observe nano-materials' characteristics, including their structure, particle size, size distribution and so on. The nanoparticle samples were pretreated before using the transmission electron microscope (JEOL-2100, JEOL Ltd). Collected and dried products are ground into powder, then a very small amount of powder was added to about 10 mL ethanol, and the particles were well dispersed in an ultrasonic water bath for 5 min. A little treated dispersion was dropped on the copper microgrid (Cu 200 mesh, JEOL) and dried. The analysis software DigitalMicrograph was used to observing the TEM images. And

more than 200 nanoparticles were counted using ImageJ software to obtain the size distribution of nanoparticles.

2.3.3 ICP Emission Spectroscopy

The concentration of Ag^+ remaining in the recovered filtrate was measured using the Inductively Coupled Plasma-Atomic Emission Spectrometer (ICP-AES) (HORIBA, JY138KH-ULTRACE).

In ICP-AES measurements, the linearity of the calibration curve is generally ensured below 40 ppm, so measurements were performed after diluting the recovered filtrate to one-tenth. After a calibration curve was prepared using a standard solution, the concentration of Ag^+ was obtained by measuring the light at the specific wavelength of the Ag element in the sample. Based on the concentration of Ag^+ remaining in the filtrate, the conversion of Ag^+ was calculated. The following equation was used to calculate the Ag reaction rate.

$$X = \left(1 - \frac{F_{out} C_{out}}{F_{in} C_{in}}\right) \times 100\%$$

where X is the reaction rate of Ag salt, F is the flow rate, and C is the Ag^+ concentration remaining in the filtrate as measured by ICP-AES.
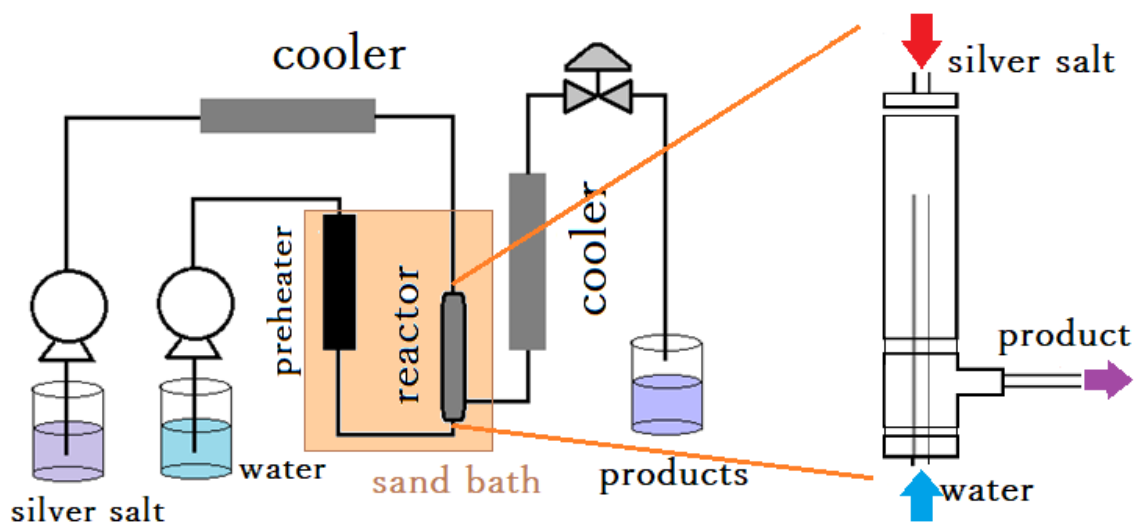
Figure 2.1 The apparatus for nanoparticles synthesis

Chapter 3 Experiment Results and Discussion

3.1 Synthesis of AgNPs at Reaction Temperature of 350°C

3.1.1 Attempts at Synthesis and the Effect of Stabilizer

According to past researches, it has been found that Ag nanoparticles can be formed in ScH_2O without reducing agents at the range of 380~430°C. To test the feasibility of the synthesis under subcritical conditions, the experiments were first performed at 350°C. The rationale for choosing 350°C as the reaction temperature was that silver can exist more stably at this temperature than silver oxide in most cases, as stated in Chapter 1, and that this temperature is closer to the supercritical temperature at which it has been shown that silver nanoparticles can be synthesized directly and successfully via CHS. Water pressure has generally not been an influential variable in past studies of the preparation of metal oxides or metal nanoparticles by supercritical hydrothermal synthesis. With reference to the experimental conditions of these studies, 25 MPa was chosen as the system pressure for all the experiments in this study. The reactor structure used in this study was referenced from the Nozzle reactor, and in the experimental design for testing this reactor, water and solution were pumped into the system at flow rates between 5 and 20 mL/min [33]. Therefore, the water-salt flow rate ratios of 10:5 and 15:7.5 were used in the experiments.

On the synthesis of silver nanomaterials using supercritical fluids, silver nitrate, silver perchlorate, silver acetate, and silver acetylacetonate have been recorded as precursor materials. Considering the research objective of making the synthesis process environmentally friendly, silver acetate was mainly used as the silver salt precursor in this study. Considering the research objective of making the synthesis process environmentally friendly, and in order to avoid the generation of toxic and complex organic substances as by-products, silver acetate was mainly used as the silver salt precursor in this study. Thus, silver acetate is dissolved in distilled water to prepare salt solution. The condition data is shown in the Table 3.1.

Although no blockage occurred in these experiments, there was still much adhesion on the wall after the reaction was completed. The inner wall of the reactor and the outer wall of the supercritical water tube inside the reactor were covered with white solids. XRD analysis of the white solid collected from the reactor wall revealed that its pattern matched the pattern of silver.

The product collected after the reaction at the outlet of the reactor was grayish brown or light yellow in water, which matches the color of the nano-silver colloid (Light yellow to dark brown, the higher the concentration, the darker the color). Then the

product was filtered and dried, and the sample obtained after that is little and sticky, making it difficult to collect a sufficient amount into the bottle. This sample with grayish-brown color was analyzed by XRD and the pattern was also consistent with the pattern of silver.

From the TEM images, the Average particle size of nano-silver is 46nm in run a1, 37nm in run a2, and Standard deviation of particle size is 19.3 in run a1, 20.4 in run a2, which shows the particle size of AgNPs is not uniform. The shapes of nanoparticles are almost all spherical, with the presence of individual rod shapes. It can be seen form the images that the nanoparticle agglomeration phenomenon is obvious (Figure 3.1).

During each experiment, the first bottle of product collected after the reaction was darker in color than the second one. It is speculated that the silver powder attached to the inner wall of the reactor first provides more attachment points for the later attached silver powder, which makes the by-product silver powder more and more with time and the outflow of the nano-silver product less and less.

In those experiments, the experimental results revealed problems of uneven particle size distribution, the presence of agglomeration, and the silver powder sticking to the reactor wall. It is speculated that the possible cause is Monolithic silver itself tends to aggregate or agglomerate. Therefore, a stabilizer Polyvinylpyrrolidone (PVP) was introduced into subsequent experiments, and its basic features have been described in section 1.4. As one of the best polymeric stabilizers for Ag nanoparticles in aqueous solutions, PVP has played the following roles according to previous research [25]:

I. It allowed higher concentrations of silver precursor to be used without silver particles sticking to the inside in the reactor.

II. It stabilized the silver particles in the product suspension.

III. It reduced the particle size distribution.

In the study by S. Kubota et al. the dispersion of copper nanoparticles synthesized with the addition of various molecular weights of PVP did not change much, but the experimental group using the highest molecular weight obtained the smallest particle size among PVP with molecular weights of 10,000, 35,000, and 40,000 [19]; therefore, PVP40 (molecular weight 40,000) was also used in this study.

In a past discussion on the thermal stability of PVP in supercritical water, there were ^{1}H-NMR analyses of PVP before and after treatment with supercritical water at 415°C and 23 MPa. The results were that the amount of monomer (N-vinylpyrrolidone) increased slightly (about 2%) after the treatment. This is due to the dissociation of the polymer chains. Therefore, in the present study, although decomposition of PVP at 350°C and 25 MPa was possible, it was presumed to be small and did not affect the experimental results and was not measured.

The experiment conditions for the introduction of this stabilizer are shown in the

Table 3.1. According to G. Aksomaityte et al.'s research, comparing to adding after the reaction, addition of PVP to the initial silver acetate solution (adding before the reaction) may perform a dual role of preventing agglomeration and increasing the conversion of Ag^+ to nanoparticle product (its -OH group may help reduce Ag^+ to Ag). In this way, the stabilizer is present during nanoparticle formation and therefore has the potential to control growth. Therefore, addition of PVP40(Mw 40000) to the initial silver acetate solution is before the reaction. However, the molar ratio used in the G. Aksomaityte et al.'s experiments is 3:1, in practice, it was found that the amount of PVP40 in this ratio was too large to be used for the preparation of raw material solutions, considering the operability and necessity of such a large number of polymers, a ratio of 1:2 was tried firstly, and then 3 ratios of PVP40 to silver acetate were also subsequently tried.

Comparing the experimental situation and results before and after the introduction of PVP, before the introduction, a lot of white silver powder was attached to the inner wall of the reactor, very little product was collected, and the first bottle of product collected after the reaction was more than the second one; whereas after the introduction, a very turbid suspension was obtained and the product collected was significantly more, in addition, the two bottles of product collected were identical in appearance. Therefore, it can be judged that the introduction of stabilizer greatly avoids the silver sticking to the wall.

The TEM images of the nanoparticles obtained with the addition of the stabilizer are shown in Figure 3.2, all 3 concentrations of stabilizers tried were effective in avoiding silver sticking to the wall so that sufficient amount of product was obtained, and the products still showed some agglomeration of nanoparticles (Similar in degree) from TEM images, but to a lesser extent than those without stabilizer. The effect of concentration of PVP40 on Ag nanoparticle size is shown in Figure 3.3 and the particle size distribution comparison is shown in Figure 3.4. The products apparently had a more uniform particle size distribution and smaller average particle size than that without stabilizer, although the difference of effect of PVP40 in the range of 5~100 g/L was not significant. This indicates that this stabilizer has the effect of preventing aggregation and preventing Ag nanoparticles overgrowth to some extent via CHS, which is consistent with previous studies.

The conversion of Ag^+ to Ag was obtained from the results of ion concentration detection by ICP-AES, and the conversion was improved from 88% to 99.7% when comparing before and after the addition of PVP. This is in agreement with the assumed results of increasing the conversion of Ag^+ to nanoparticle product.

3.1.2 Effect of Residence Time

In a study on continuous hydrothermal synthesis of cobalt oxide nanoparticles, they

found that an increase in residence time (across 0.4 and 8 s) results in increasing nanoparticle size regardless of reaction temperature. That can be interpreted as that in reaction process, if residence time is longer, the growth time of particles is longer, then larger particles will tend to form. And in their study, the effect of residence time on conversion is most pronounced at lower reaction temperatures (200-330 °C) [34].

The structural characteristics of the reactor used in this study make it difficult to vary the residence time by changing the length of the reactor. Therefore, experiments with different residence times (limited time frame) were attempted by scaling up or down the flow rates of supercritical water and salt solutions equivalently (shown in Table 3.2).

The Ag nanoparticle sizes of these experiments with different residence time are shown in Figure 3.5. The effect of residence time in the frame of 1.5~4.5s is not significant, after the reaction time exceeded 4.5 s, there was a slight increase in the average particle size, which exceeded 30 nm. The conversion rates were all higher than 99.5% after a retention time of more than 3s. In the experimental group with a residence time of 1.5 s, the conversion rate was 98.3%, a slight decrease.

The time dependence is not reflected, perhaps because the reactions have been carried out thoroughly in this time frame, or the effect of residence time needs to be manifested at lower temperatures (cf. the synthesis of cobalt oxide described).

3.1.3 Effect of precursor concentration

In previous studies on the preparation of metal oxide nanoparticles by supercritical hydrothermal synthesis, an increase in the particle size of the product nanoparticles with increasing concentration of the metal precursor solution has been observed several times. In the preparation of Fe_2O_3 nanoparticles by supercritical hydrothermal synthesis by Sue et al. [35], the average particle size and the coefficient of variation increased with increasing $Fe(NO_3)_3$ molality. In a study of synthesis of zirconia nanoparticles, the crystallite size and particle size of the product increased with the precursor concentration [36]. But there is also opposite result: in the study of synthesis of cobalt oxide nanoparticles, the lower the concentration of the precursor, the larger the particle size tends to appear [38]. Therefore, specific analysis is necessary for the synthesis of different nanoparticles.

On the other hand, about the researches about synthesis of metal nanoparticles, there are the following results: in the study by Zhou et al. [32], via supercritical hydrothermal synthesis, when the concentration of copper sulfate increased (0.05 to 0.5 mol/L), the average particle size of the copper nanoparticles increased (14 to 50 nm). In Zhou et al.'s experiments, solid products at high precursor concentrations caused clogging of the tubing in the reaction system, so they had to switch to a batch-type reactor to complete their experiments. To avoid a similar situation, the reaction concentrations

designed in this study ranged from 0.0025 to 0.03 mol/L.

Experiments for the synthesis of mental silver nanoparticles were also carried out at 350 °C using the concentration of silver acetate precursor solution as a variable. Experiment conditions are shown in Table 3.2. The residence times were all around 3.0 s.

The effect of precursor concentration on average Ag nanoparticle size is shown in Figure 3.6. According to the average particle size, when the concentration of silver salt solution is higher than 0.01mol/L, the average particle size increased compared with 0.005mol/L, but continuously increasing or reducing precursor concentration did not have a significant effect. And from the corresponding TEM images, it can be observed that the higher the precursor concentration, the greater the tendency for larger nanoparticles to appear. This may be due to the fact that at higher concentrations, i.e., high initial supersaturation (then it will drop), though the nucleation rate is higher, the primary nucleation stage is shortened and the initial growth rate is also higher [37]; in addition, during the growth period of particles, the precursor ions are still at a not-so-low concentration, then the growth time of particles won't be limited, thus the particles could get more fully grown (The crystalline size depends on the ratio of the nucleation to the growth of crystals).

The particle size distribution of the products obtained with different precursor concentrations is shown in Figure 3.7. The bar graphs of the particle size distribution shows that the breadth of the particle size range increased with increasing concentration, although the distribution peaks at precursor concentrations of 0.01, 0.02, and 0.03 mol/L are in a similar particle size range. When the precursor concentration is 0.0025 mol/L, the particle size distribution is the narrowest and particles with particle size over 60 nm hardly appear. It indicates that the crystallization kinetics of AgNPs may be influenced by precursor concentration. At low silver salt concentration, primary nuclei were generated rapidly, which greatly reduced the concentration of silver ion and thus suppressed the secondary nucleation (a type of heterogeneous nucleation); And the growth of AgNPs was limited, then the nanoparticles with uniform particle size were obtained. Whereas, at high silver salt concentration, the secondary nucleation was likely to occur, so nucleation and growth happened at the same time, which resulted in wide distribution of AgNPs.

In this series of experiments, the conversion rates from Ag^+ to Ag are all above 99.4%.

3.1.4 Effect of Flow Rates Ratio of ScH₂O: Silver salt

In past studies of continuous hydrothermal synthesis, few reports have been seen in which the flow rate ratio was used as a variable and its effect on the products was explored. In the synthesis of copper nanoparticles by S. Kubota et al. the ratio of the

flow rate of water (to which a reducing agent was added) to the flow rate of the precursor solution seems to have an effect on the particle size of the product. While keeping the total flow rate consistent, they tried two sets of experiments with different flow rate ratios (45:15 and 40:20). The experimental results showed that decreasing the ratio of reducing agent stream to precursor stream flow rate could lead to small particle diameters and small crystallite sizes. To further investigate whether the water-salt flow rate ratio plays a role in controlling the particle size of metal nanoparticles, in this study, the water-salt flow rate ratio was chosen as the variable and the total flow rate was kept at 20 mL/min, and the experiment conditions are shown in Table 3.2. The residence times were all around 3.3s.

The product particle sizes of the experimental groups with different flow rate ratios are shown in Figure 3.8. As the proportion of water stream decreased and the proportion of salt solution stream increased, the average particle size of nanoparticles showed a trend of decreasing and then increasing. The decreasing trend may because the increased flow rate of salt results in the higher degree of supersaturation, which leads to smaller particle size [19]; On the other hand, the reason of the increasing trend may be that the water was heated, its reduced proportion corresponds to a lower heating rate of the salt solution, which slows down the reaction rate and makes the particle size increase. Figure 3.9 shows the particle size distribution for different flow rate ratios. From this figure, it can be seen that as the flow rate ratio of supercritical water stream to silver salt solution stream decreased from 3:1 to 2:1, not only the peak moved towards the direction of small particle size, the range of particle size distribution is also obviously narrowed, presenting a more desirable particle size distribution; when the flow rate ratio continued to decrease from 2:1 to 1:1, the peak moved towards the direction of large particle size, and the range of particle size distribution became wider.

In this series of experiments, the conversion rates from Ag^+ to Ag are all above 99.4%.

3.2 Synthesis of Ag nanoparticles at lower temperature

Direct preparation of silver nanoparticles at lower temperatures by continuous hydrothermal synthesis in the absence of reducing agents has not been reported in any researches. From the results and conversion (above 98%) of the aforementioned experiments conducted at 350°C, it is likely that direct production of silver nanoparticles at lower temperatures is feasible.

The one-step synthesis of silver nanoparticles using silver acetate solution as a precursor was tried in the range of 220~350°C. The experimental conditions are shown in Table 3.2. Since the density of ScH_2O changes with Temperature, the flow rates were adjusted slightly to keep the residence time at about 3s when Temperature changes.

As shown in Figure 3.10, it was confirmed that metal Ag was obtained at 350, 325, 275, 245, 235°C by XRD patterns of the products. All of the products in this series of experiments matched the standard pattern of [Silver-3C, syn] with cubic crystal system, which is the most common type of silver structure. The crystallite size of product silver nanoparticles of each group can be obtained based on XRD data and the results are shown in Figure 3.11. According to the TEM images, the particle sizes of the products obtained at different reaction temperatures are shown in Figure 3.12. The average nanoparticle size and crystallite size both have a tendency to decrease with decreasing temperature. The tendency of the particle size of the synthesized silver nanoparticles to decrease with decreasing temperature can be visualized from the TEM images (Figure 3.13). This is contrary to the result that higher temperatures led to smaller Ag nanoparticles in supercritical condition [23]. Above the supercritical point, the solubility of the metal Ag precursor in water decreases rapidly with increasing temperature, which may lead to the production of a large number of nuclei in a short period of time, thus limiting the growth of the nanoparticles, and making the particle size smaller. But in the subcritical condition, in the temperature range of 230 to 350°C tried in this study, which is not close to the critical point of water, the precursor solubility increases with increasing temperature and therefore the degree of supersaturation decreases, thus fewer nuclei are formed during the nucleation stage, and the silver ions remaining in solution after nucleation may be consumed for particle growth instead of generating new nuclei, which makes the product particles grow to a greater extent. In addition, elevated temperatures may accelerate the growth of the particles during the growth stage.

Figure 3.14 illustrates the particle size distribution of silver nanoparticles synthesized at 325°C, 300°C, 275°C, 235°C, 225°C and 220°C. At temperatures between 350 ~ 235°C, the particle size distribution of the product has only one peak. However, in the experiments at 225 and 220°C, the particle size distribution of the product particles was concentrated in two ranges, resulting in very large standard deviations, which indicated the presence of both smaller and larger particles. Consequently, this also increases the average particle size of silver nanoparticles obtained below 225°C. This phenomenon can be seen more visually on the TEM images (Figure 3.13), at the reaction temperature of 235 °C, the product nanoparticles showed small and uniformly distributed particle sizes, better than higher temperature experimental products. But at the reaction temperature of 225 °C, both smaller and larger particles appeared. Another related phenomenon that occurred when nano-silver is synthesized below 225 °C is that very small number of giant particles (300~400 nm) appeared in the experimental product at 225°C and 220 °C (Figure 3.15). The interplanar crystal spacing of the giant particle was obtained from the HRTEM image, two sets of crystal plane spacings were obtained

after calibrating the diffraction pattern produced after the Fourier transform. They are $d_1 = 0.2314$ nm and $d_2 = 0.2002$ nm, which correspond to (1,1,1) and (2,0,0) crystal planes when compared with the standard card of [Silver-3C, syn]. It revealed that it is still metallic silver like other small particles. That is, although the crystallite size of silver nanoparticles is smaller at a certain lower temperature, overgrown particles also appear in the product. It is likely that abnormal grain growth, which also referred to as secondary recrystallisation, occurred. Abnormal grain growth is a grain growth phenomenon through which certain energetically favorable grains grow rapidly in a matrix of finer grains resulting in a bimodal grain size distribution, and it is characterized by the growth of most grains being stunted while a very small number of grains grow rapidly [39]. When the number of boundaries of a grain is greater than the number of boundaries of neighboring grains, the curvature of these grain boundaries increases, and the driving force of grain boundary migration increases accordingly, the growth of the grain is faster than that of the surrounding small grains, and therefore the small grains are engulfed and the large grain formed [40]. There are many reasons for inducing abnormal grain growth, but they are generally present during the calcination process. The similar phenomenon when synthesizing silver nanoparticles below 225°C might because that at lower synthesis temperatures, the newly formed silver grains are more sensitive to fluctuations in the reaction temperature (experimental error), and this conjecture that requires more evidence and future probing.

The effect of temperature on silver ion conversion is shown in Figure 3.16. Obviously, the conversion rates of Ag^+ decreased with decreasing temperature below 300°C. Increasing reaction temperatures result in a higher conversion, which is in agreement with the results of previous studies on the synthesis of metal oxide nanoparticles.

3.3 Attempts at different precursors

Compared to the solubility of silver acetate at room temperature, silver nitrate is much more soluble at room temperature. Considering theoretically, high-temperature and high-pressure water circumstance will reduce the solubility of inorganic salts, but the solubility of silver nitrate will still be higher than that of silver acetate in comparison. In addition, silver nitrate has better thermal stability than silver acetate. As mentioned in chapter I, the only reported study of supercritical hydrothermal synthesis with silver nitrate as a raw material used glycerol as a reducing agent and ended up with a product silver with a very large particle size. It can be assumed that the synthesis experiment of nanomaterials was not considered a success.

To investigate the different possibilities of synthesizing silver nanoparticles, experiments were carried out using silver nitrate as a precursor solution, the conditions

are shown in Table 3.3.

In the experimental group where no stabilizer was added, the product is clear liquid and its pH is 7, and precipitation occurs after adding NaCl and NaOH solution, and no silver attached to the wall of the reactor. And then, based on the measured ion concentration in the clear product liquid, the conversion of Ag^+ was calculated to be only 14.2%. Therefore, it can be judged that under such experimental conditions, silver nitrate hardly reacts. In the experiments with added PVP, only a very small amount of product was obtained in both sets of experiments at 350°C and 370°C. The product liquid pH is 5, and its color turned darker after adding NaOH. After TEM analysis, the products can be seen on the images with only a small amount of shapeless nanostructures (Figure 3.17). In other words, the synthesis of silver nanoparticles under subcritical conditions using silver nitrate as a precursor does not work.

3.4 Treatment of Ag_2O in subcritical water in batch system

Actually, no previous studies have been recorded on the direct conversion of Ag_2O to Ag in supercritical or subcritical water. As stated in Chapter 1, it is assumed that silver salts are first converted to silver oxide and then to silver nanoparticles in a hydrothermal synthesis reaction. However, in the experiments with temperature as the variable, there was still no silver oxide when the temperature was lowered to about 220°C. Therefore, two experiments were conducted to investigate the presence of silver oxide as an intermediate product in the preparation of silver nanoparticles, using silver oxide powder as raw material in a batch reactor (Table 3.4).

The XRD patterns of the products showed that Ag_2O did not decompose to Ag in these experiments (Figure 3.18). It is possible that there is no step of thermal decomposition of Ag_2O in the continuous hydrothermal synthesis of nano-Ag, or nano-Ag can only be synthesized under subcritical conditions using salt solutions as raw materials rather than Ag_2O.

Table 3.1 Experimental Conditions (a)

	T(°C)	P(MPa)	Concentration of CH_3COOAg (mol/L)	Flow rates for scH_2O: silver salt (mL /min)	Molar ratio for PVP40: silver salt	Average particle size (nm)
a1	350	25	0.005	10:5	0	46
a2	350	25	0.005	15:7.5	0	37
a3	350	25	0.005	15:7.5	1:2	26
a4	350	25	0.005	15:7.5	1:10	26
a5	350	25	0.005	15:7.5	1:20	27
a6	350	25	0.005	15:7.5	1:40	28

#Concentration and flow rates are all in ambient state.

Table 3.2 Experimental Conditions (b~e)

	T(°C)	P(MPa)	Concentration of CH₃COOAg (mol/L)	Flow rates for scH₂O: silver salt (mL /min)	Molar ratio for PVP40: silver salt
e1	350	25	0.005	10:5 (t: 4.5 s)	1:20
e2	350	25	0.005	13.3:6.7 (t: 3.3 s)	1:20
e3	350	25	0.005	15:7.5 (t: 3.0 s)	1:20
e4	350	25	0.005	10:5 (t: 4.5 s)	1:20
b1	350	25	0.0025	15:7.5	1:20
b2	350	25	0.005	15:7.5	1:20
b3	350	25	0.01	15:7.5	1:20
b4	350	25	0.02	15:7.5	1:20
b5	350	25	0.03	15:7.5	1:20
c1	350	25	0.005	15:5	1:20
c2	350	25	0.005	14.3:5.7	1:20
c3	350	25	0.005	13.3:6.7	1:20
c4	350	25	0.005	12:8	1:20
c5	350	25	0.005	10:10	1:20
d1	350	25	0.005	15:7.5*	1:20
d2	325	25	0.005	15:7.5*	1:20
d3	300	25	0.005	15:7.5*	1:20
d4	275	25	0.005	15:7.5*	1:20
d5	245	25	0.005	15:7.5*	1:20
d6	235	25	0.005	15:7.5*	1:20
d7	225	25	0.005	15:7.5*	1:20
d8	220	25	0.005	15:7.5*	1:20

#Concentration and flow rates are all in ambient state.
* When T was the variable, the flow rates were adjusted slightly to keep the residence time at about 3 s.

Table 3.3 Experimental Conditions (g)

	T($^\circ$C)	P(MPa)	Concentration of AgNO$_3$(mol/L)	Flow rates for scH$_2$O: silver salt (mL /min)	Molar ratio for PVP40: silver salt
g1	350	25	0.005	15:7.5	0
g2	350	25	0.005	15:7.5	1:20
g3	370	25	0.005	15:7.5	1:20

#Concentration and flow rates are all in ambient state.

Table 3.4 Experimental Conditions in Batch Reactor (f)

	T($^\circ$C)	Precursor	Residence Time
f1	250	Ag$_2$O powder	30 min
f2	300	Ag$_2$O powder	30 min
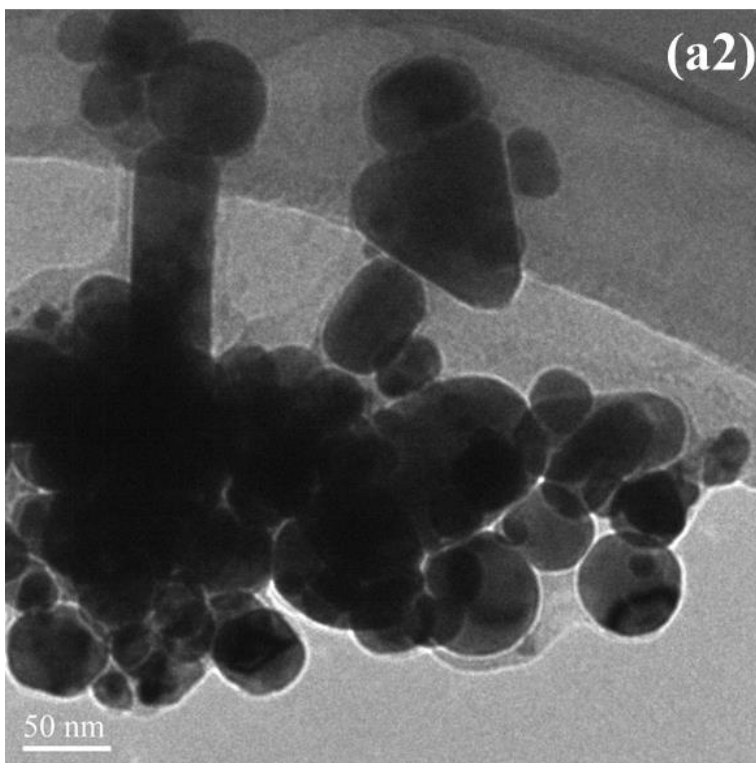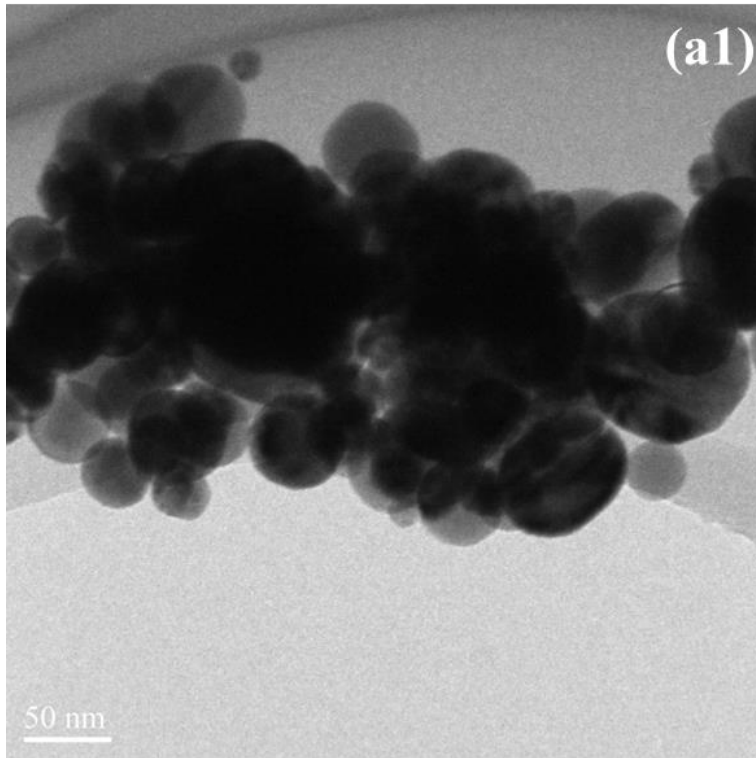
Figure 3.1 TEM images of product in a1, a2 without stabilizer
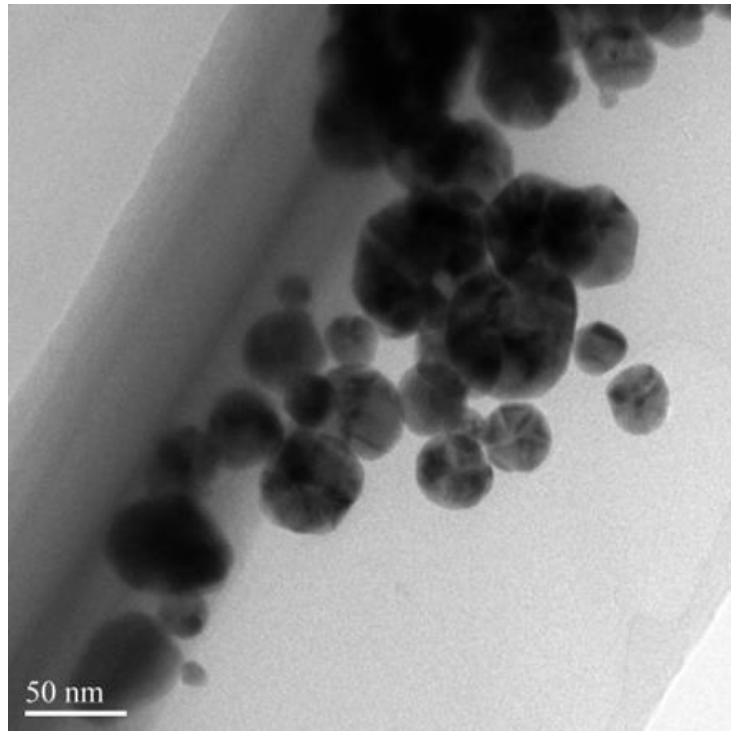
Figure 3.2 TEM image of product with PVP40 in a5
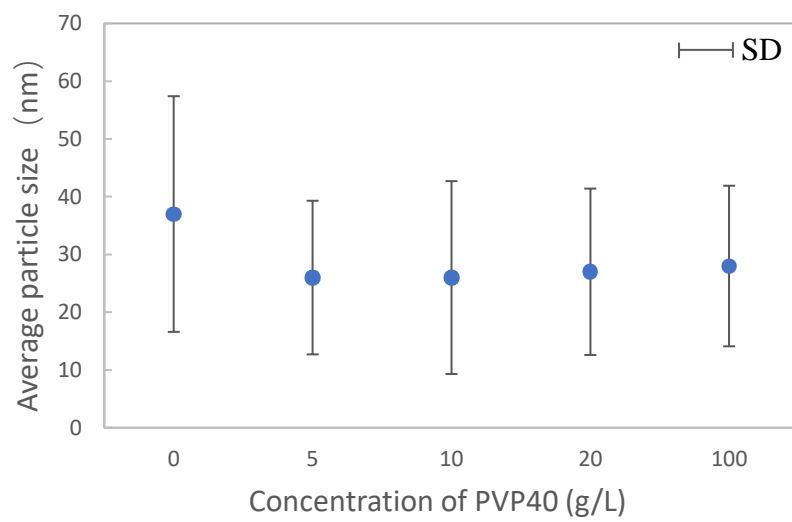
Figure 3.3 Effect of concentration of PVP40 on Ag nanoparticle size
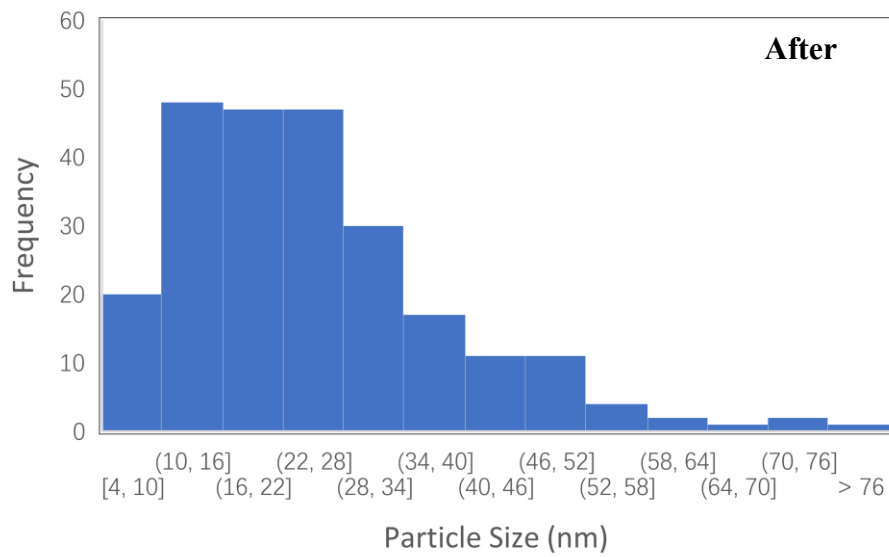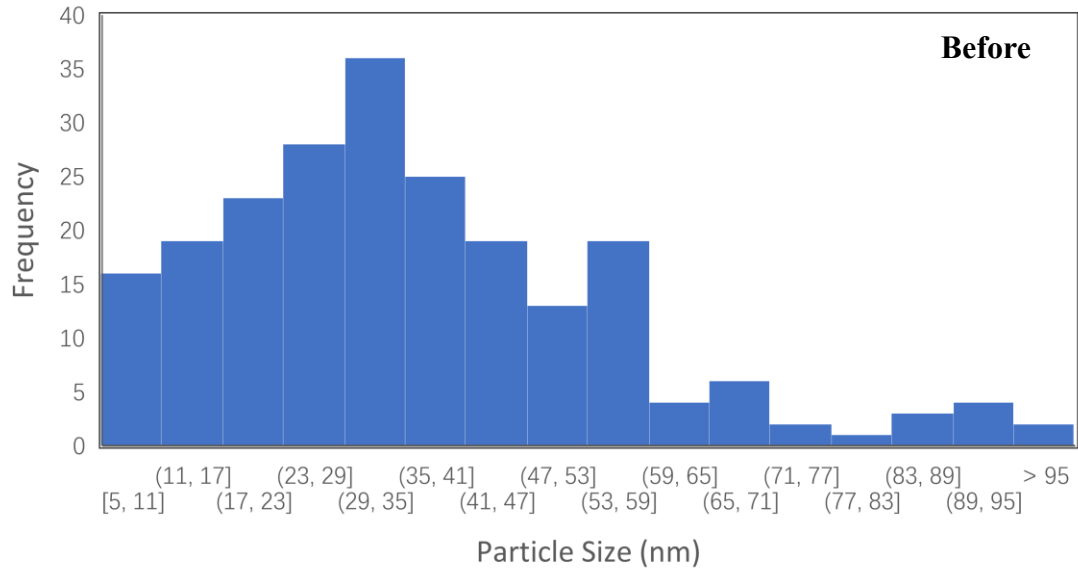
Figure 3.4 Comparison of particle size distribution of products before and after adding stabilizer
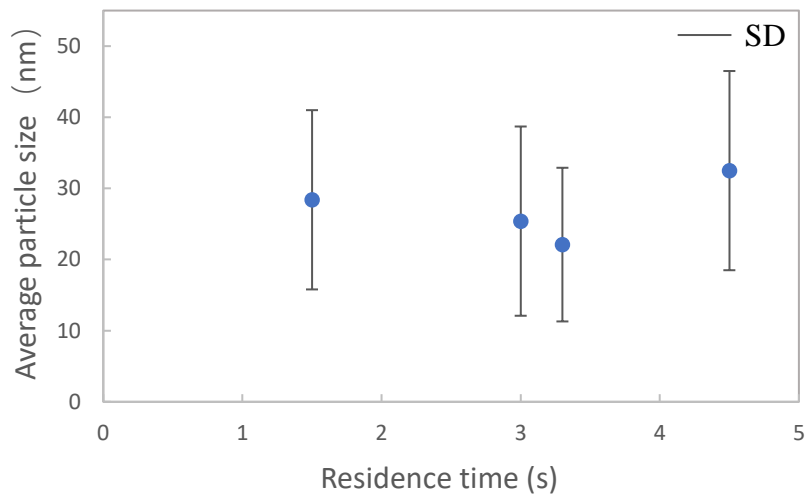
Figure 3.5 Effect of residence time on Ag nanoparticle size
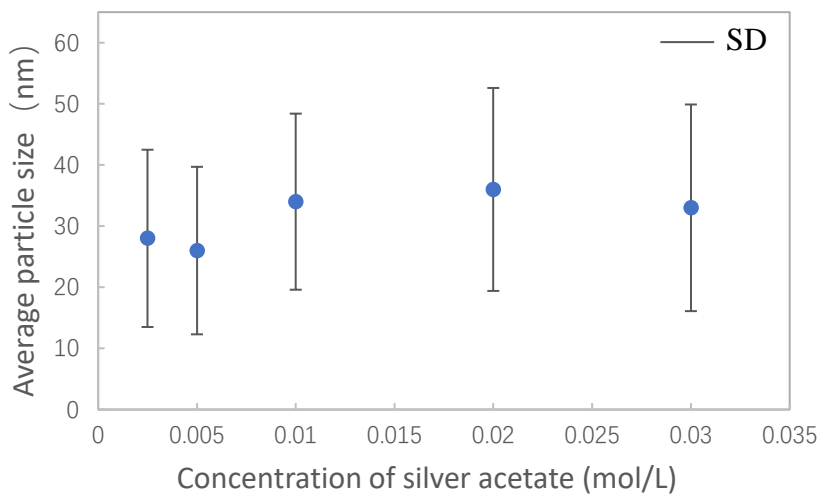
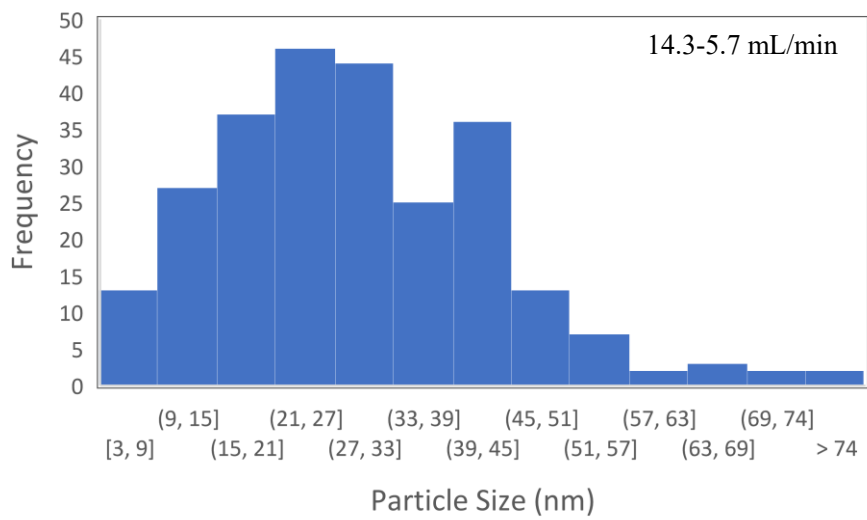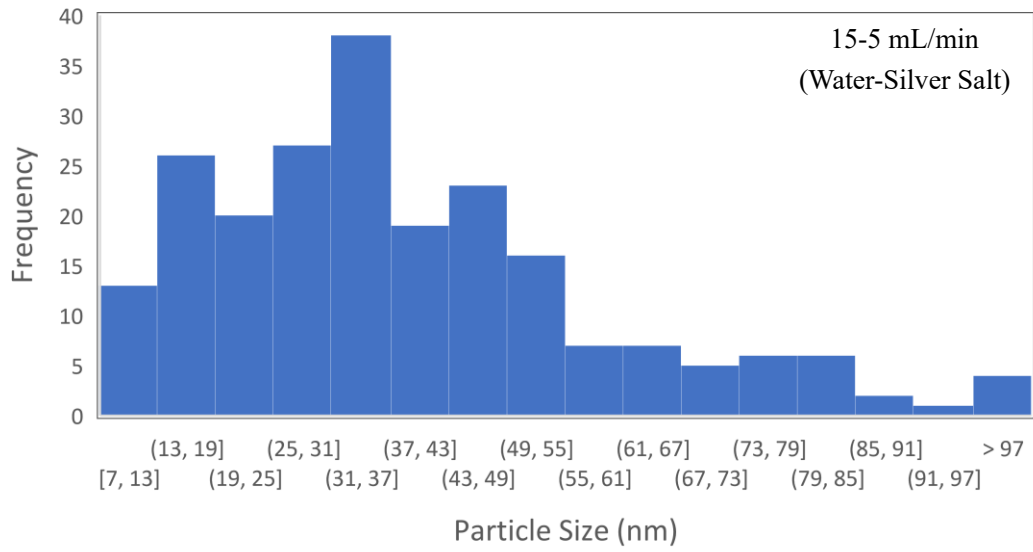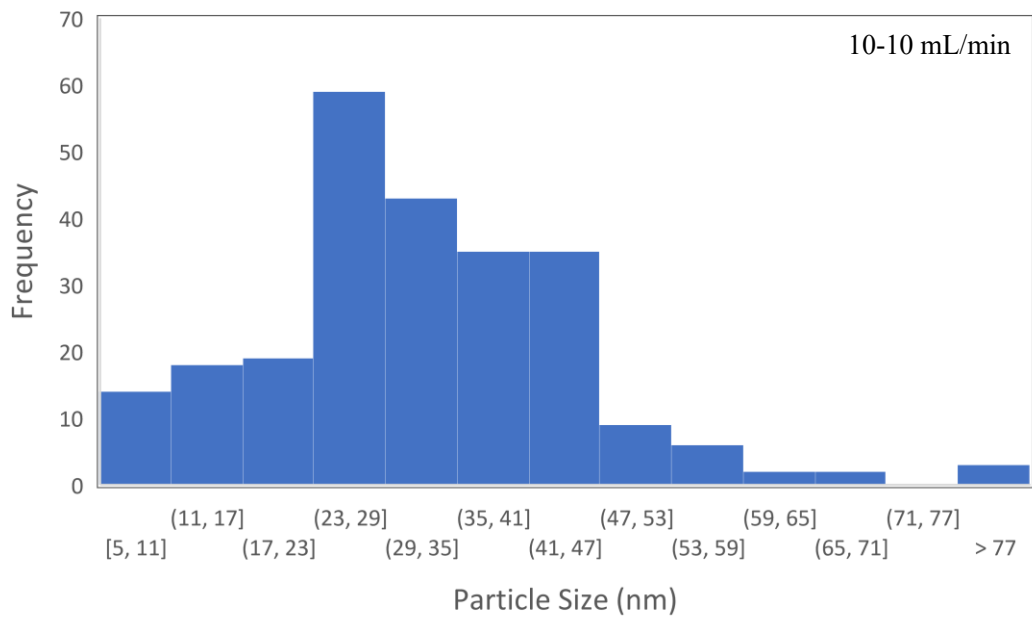**Figure 3.6 Effect of precursor concentration on Ag nanoparticle size**
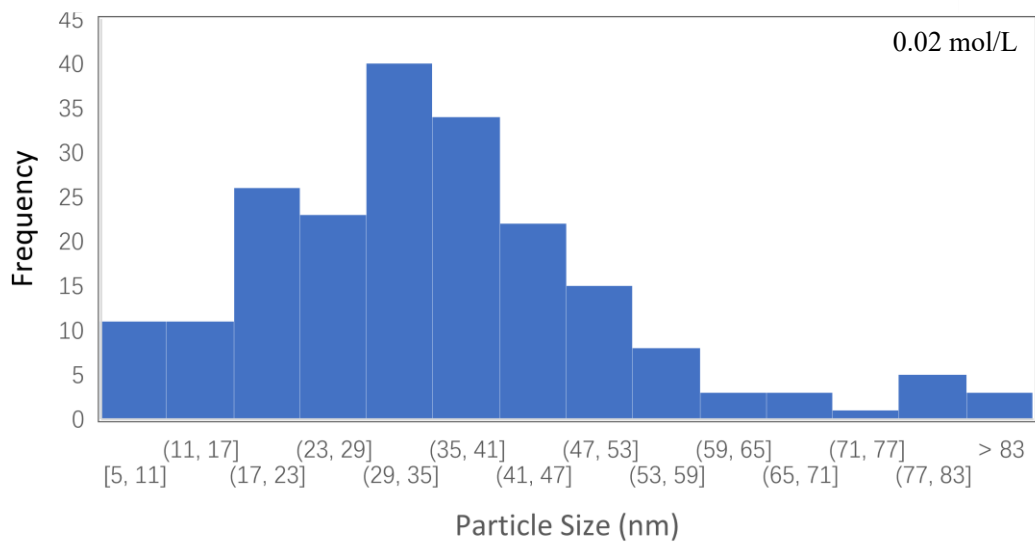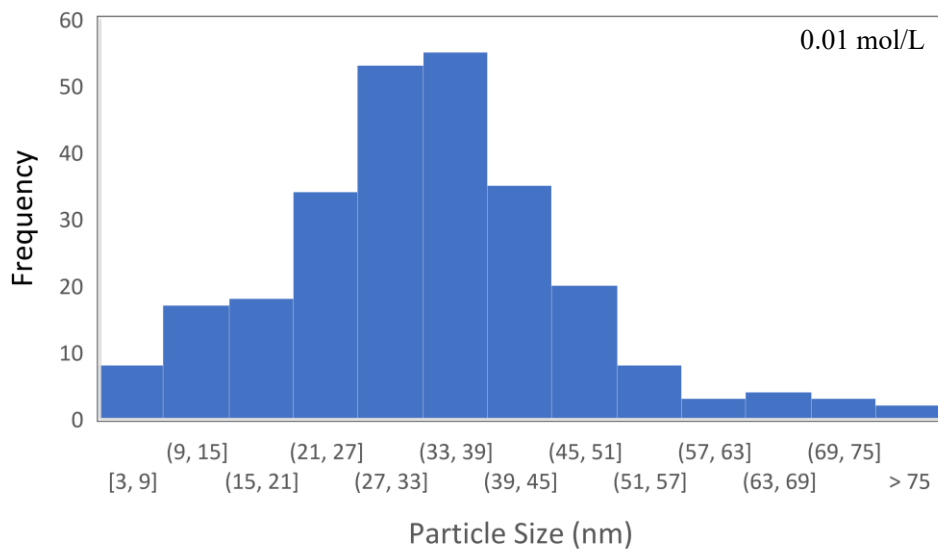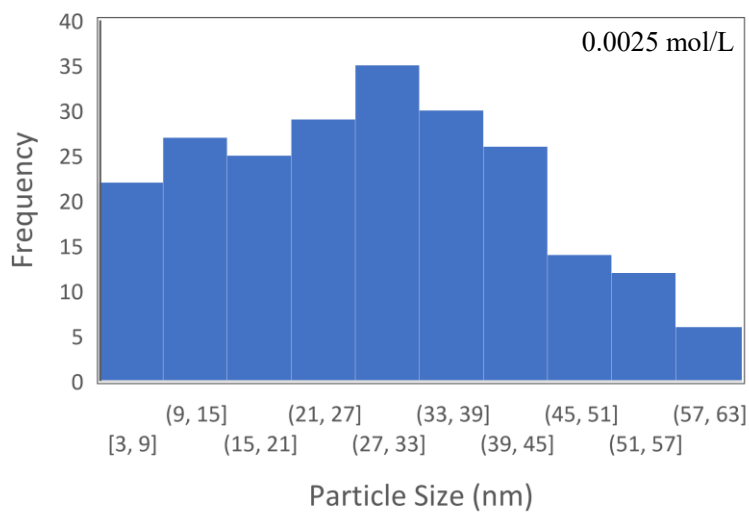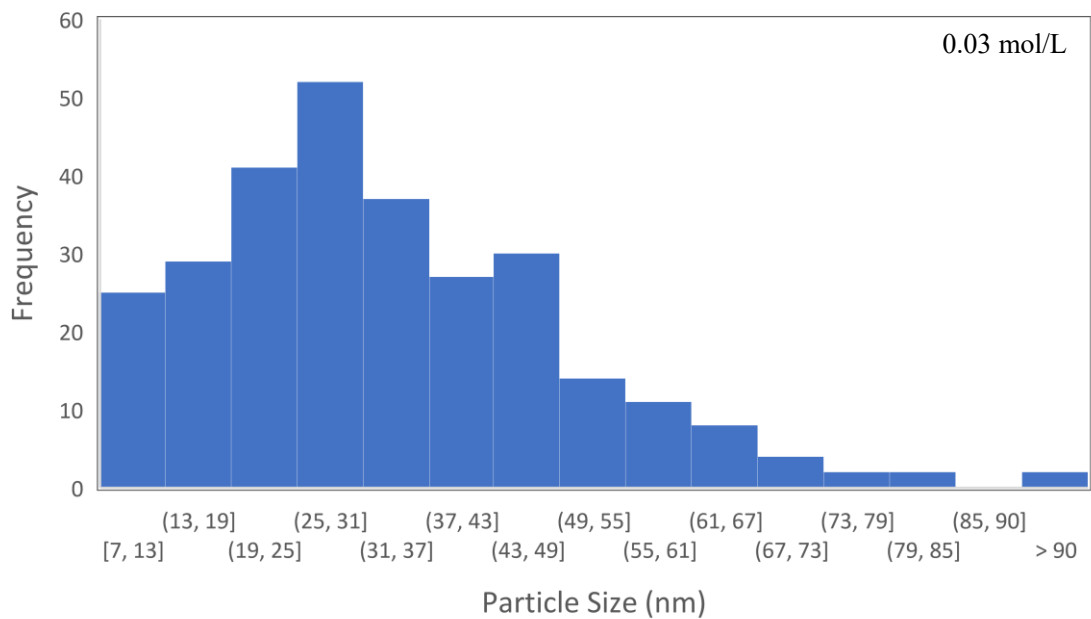
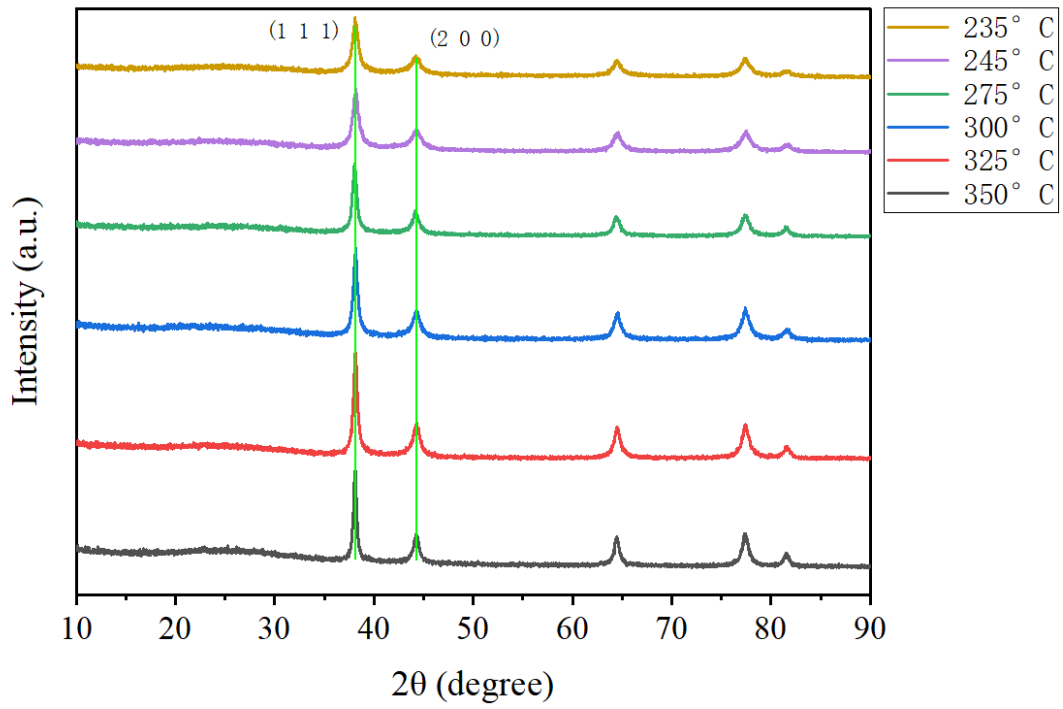**Figure 3.7 Particle size distribution for different precursor concentrations**
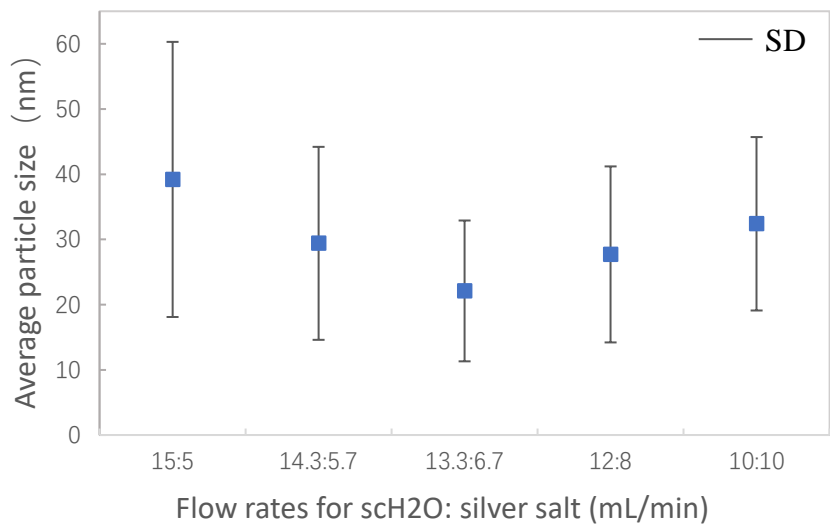
Figure 3.8 Effect of flow rates ratio on Ag nanoparticle size
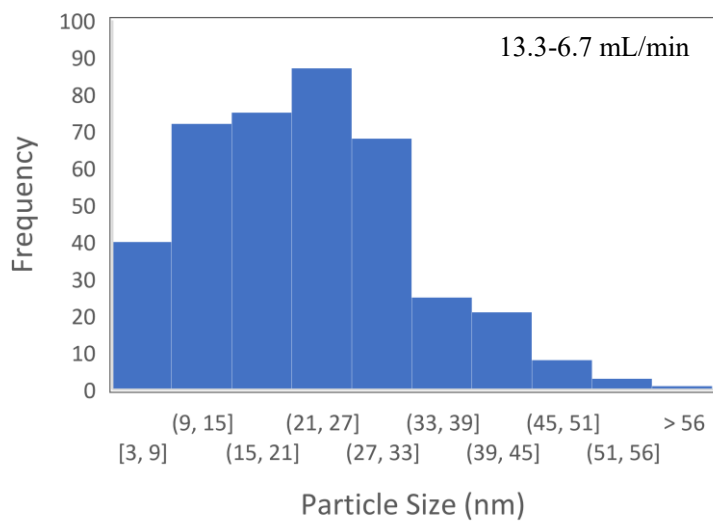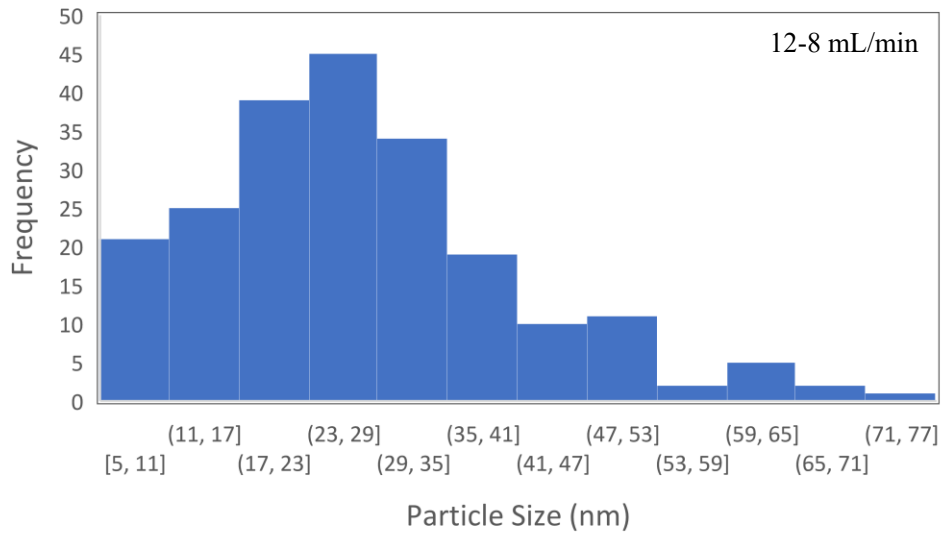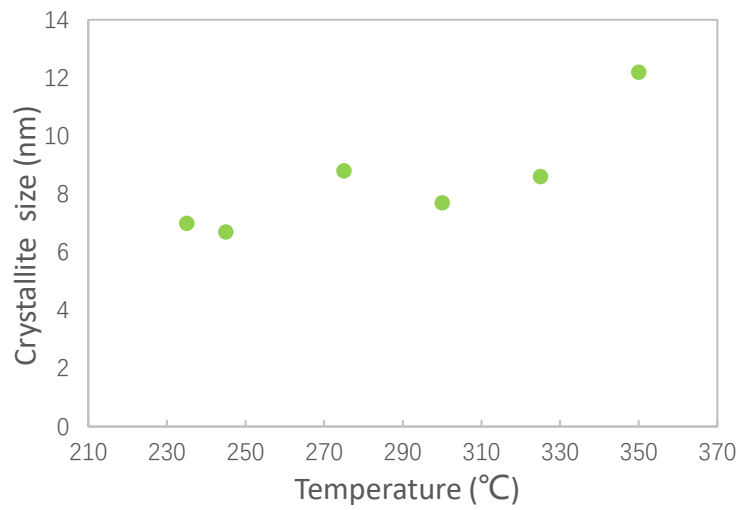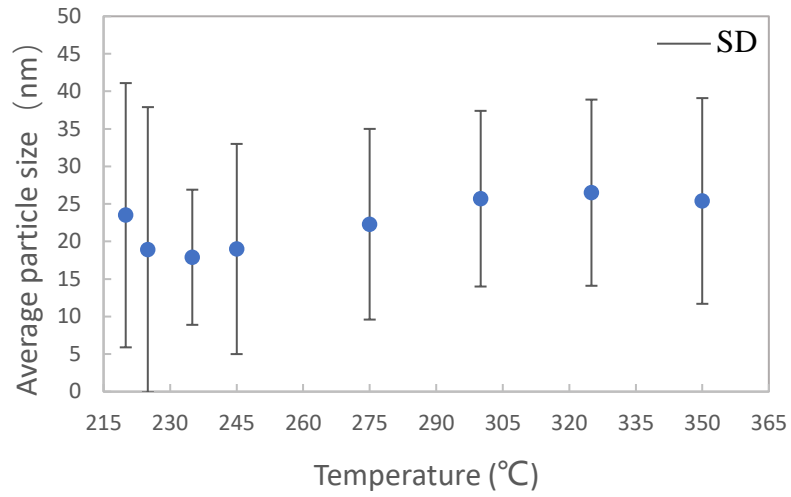
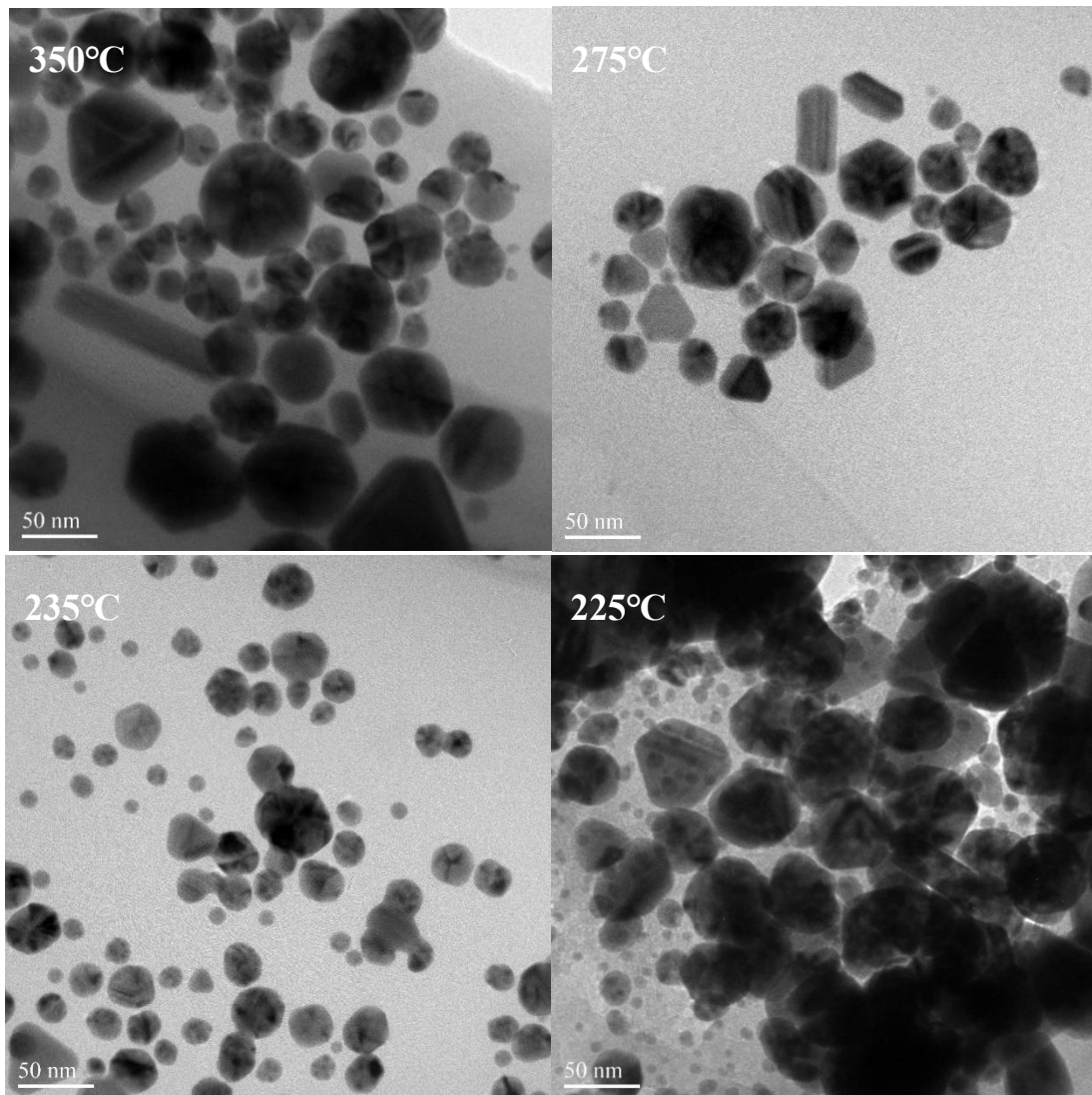**Figure 3.9 Particle size distribution for different flow rate ratios**
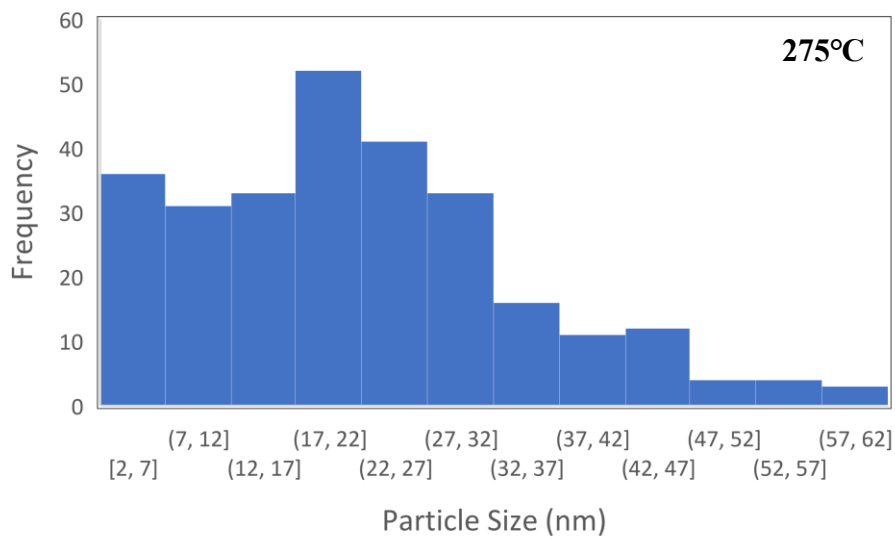
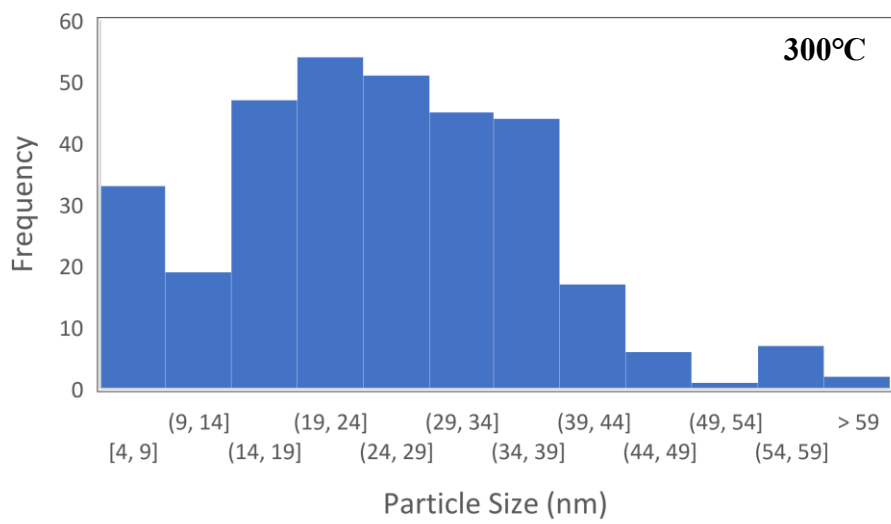**Figure 3.10 The XRD Pattern of products**

Figure 3.11 Effect of temperature on Ag crystallite size

Figure 3.12 Effect of temperature on Ag nanoparticle size

Figure 3.13 TEM images of product at 350℃, 275℃, 235℃ and 225 ℃
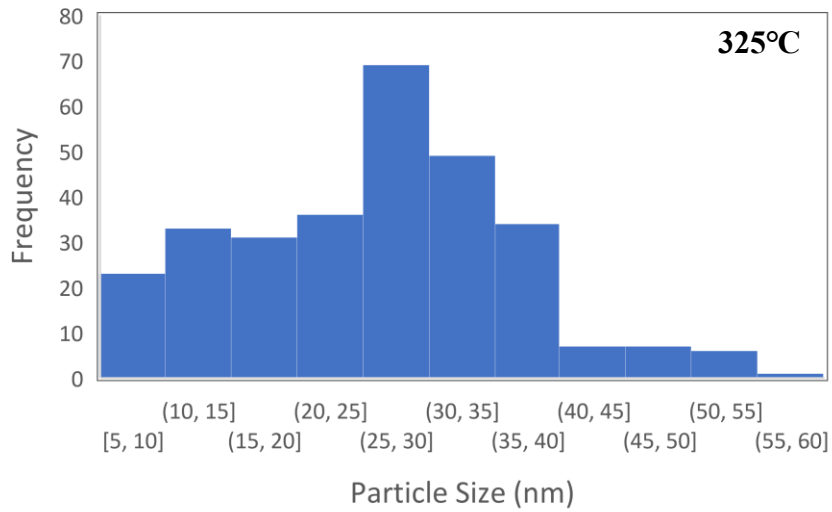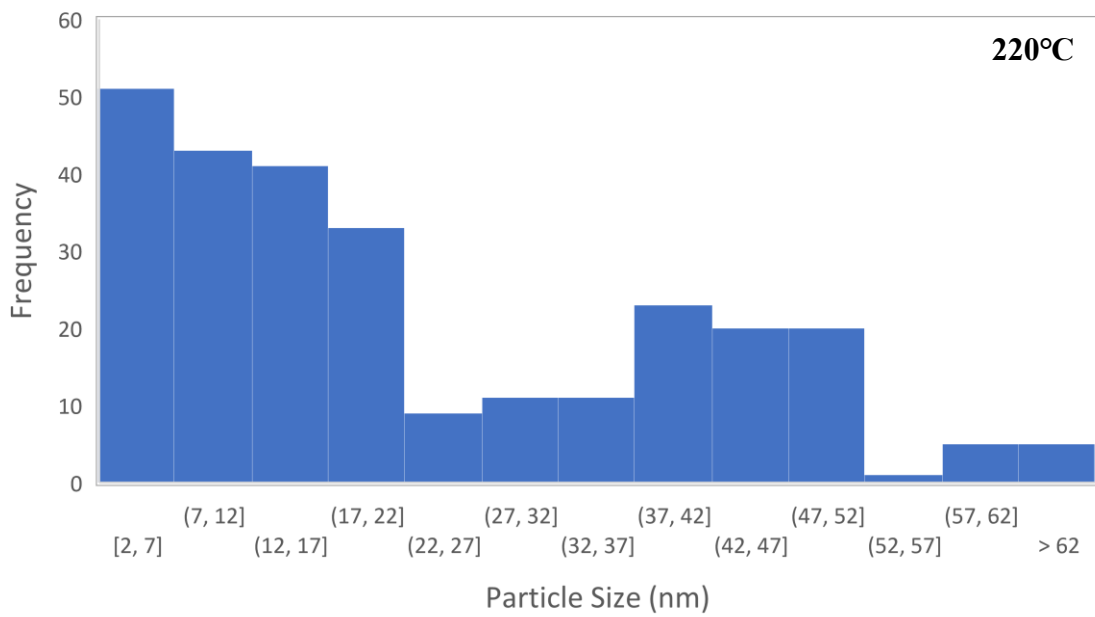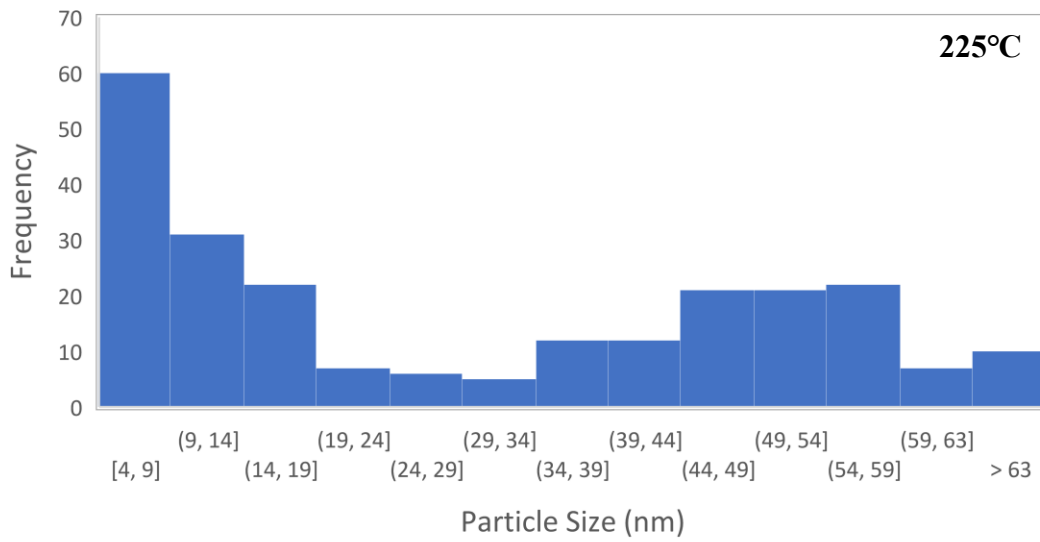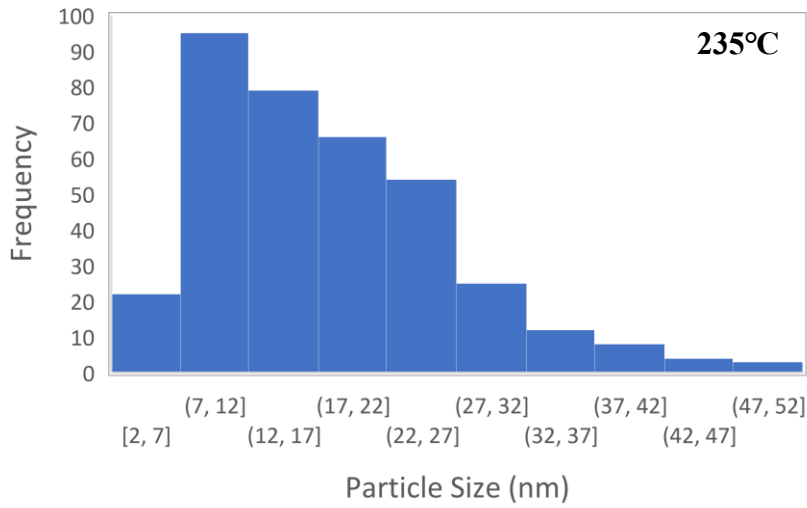
Figure 3.14 Particle size distribution at different temperature

220°C

0.2 μm

225°C

100 nm

Figure 3.15 TEM images of product at 220°C and 225°C
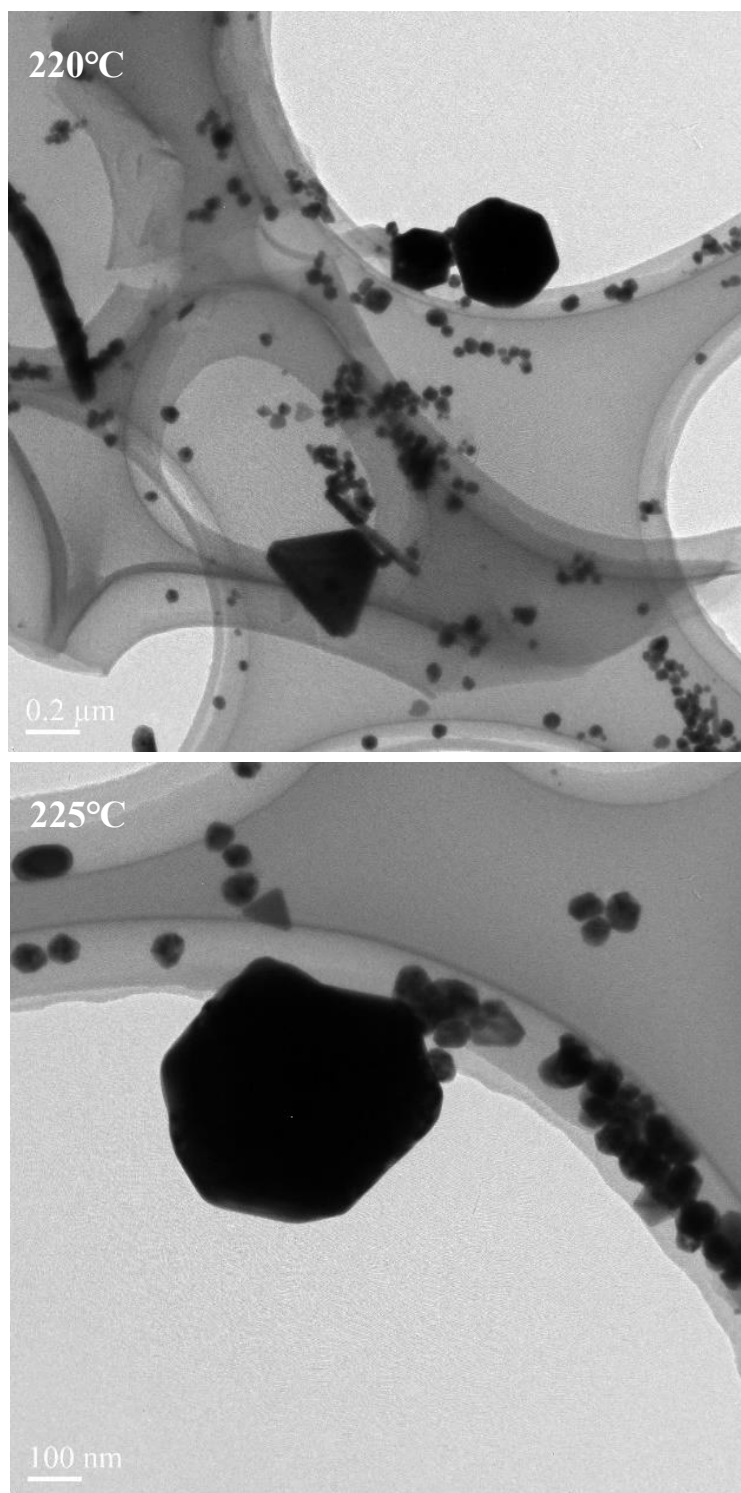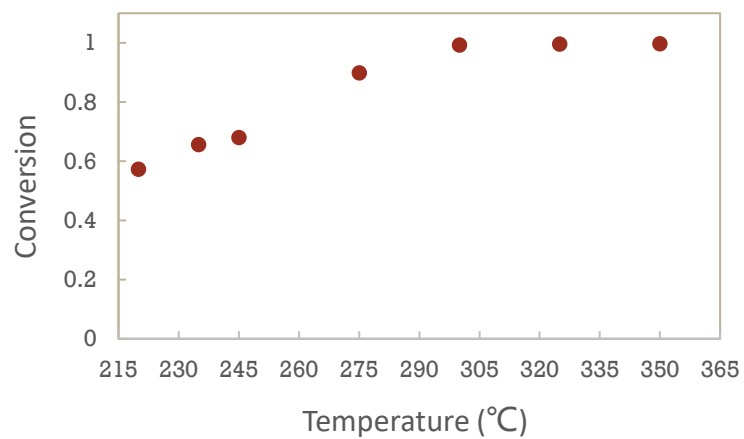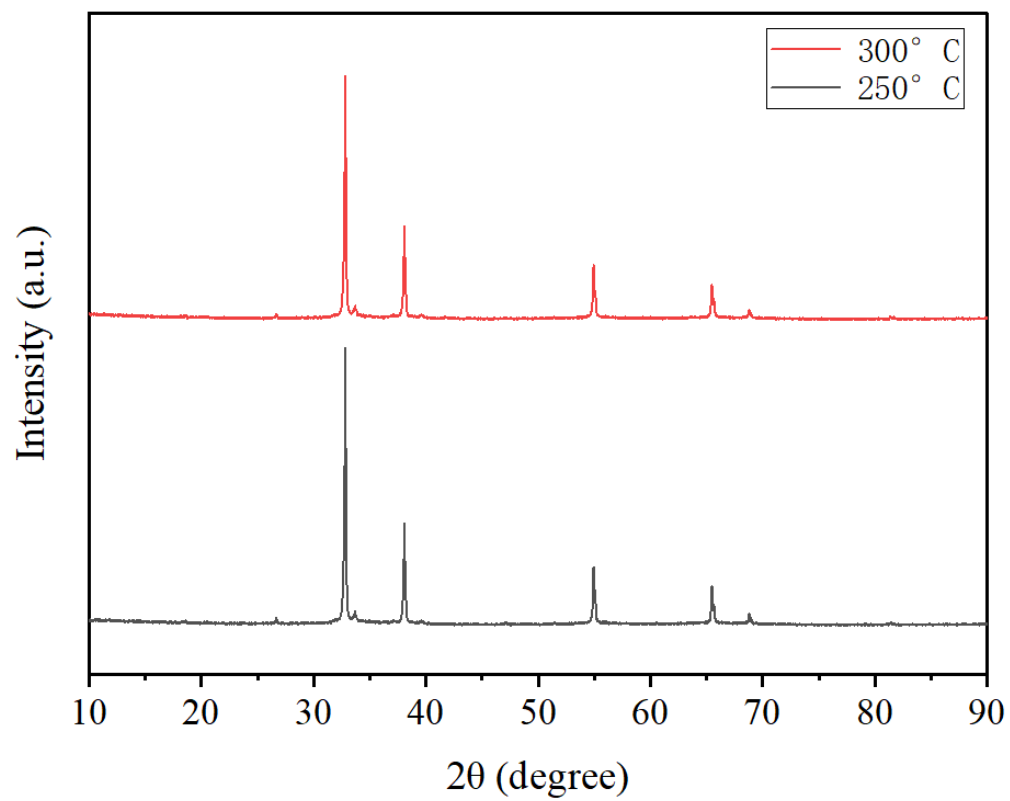
Figure 3.16 Effect of temperature on silver ion conversion
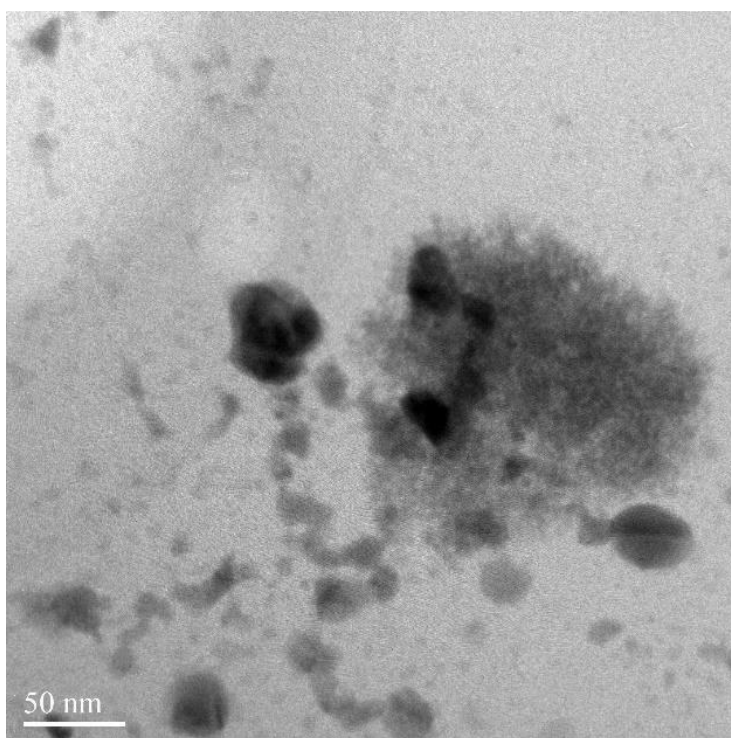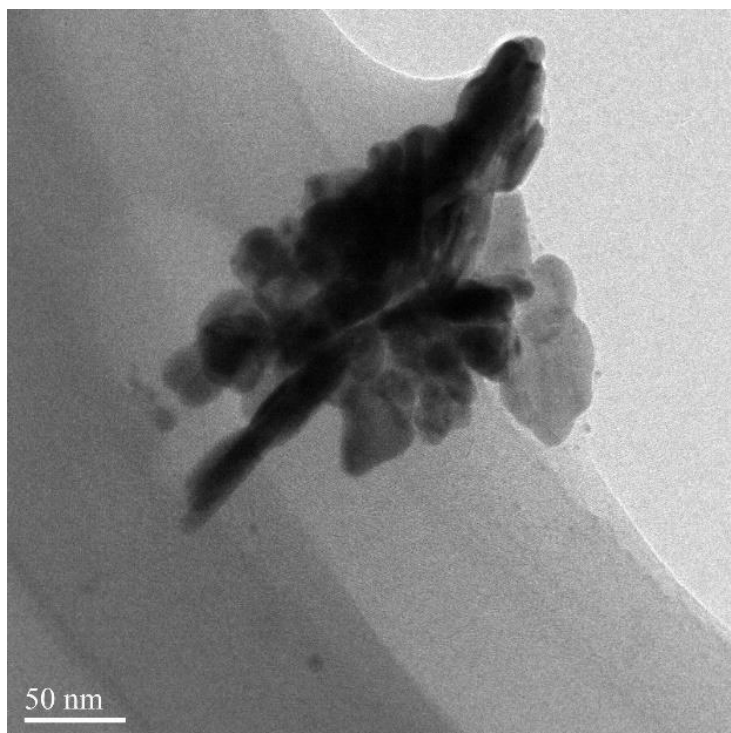
Figure 3.17 TEM images of product using AgNO₃ as precursor

Figure 3.18 The XRD Pattern of Ag$_2$O treated at 250 or 300°C

Chapter 4 Conclusion and Prospect

4.1 Summary and Conclusion

In this study, AgNPs were successfully synthesized in one step by continuous hydrothermal synthesis under subcritical conditions without the use of reducing agent. The particle size, size distribution, morphology, and conversion of the synthesized nanoparticles were evaluated in the investigation of size controllable synthesis of Ag nanoparticles. The results explored for different parameters are as follows: The addition of stabilizer PVP40 is effective in preventing particle aggregation, preventing AgNPs overgrowth (Average particle size: from 37 to 27 nm, SD: from 20 to 15), and increasing the conversion (from 88% to 99.7%). And the reduction of precursor concentration was effective in reducing the particle size (from 36 to 26 nm) and narrowing the particle size distribution (SD: from 17 to 14). The time dependence for particle size in the frame of 1.5~4.5 s was not significantly reflected. When flow rates ratio of ScH_2O to salt solution was the variable, as the proportion of water stream decreased and the proportion of salt solution stream increased, the average particle size showed a trend of decreasing and then increasing (from 39 to 22 nm, then to 32 nm), and the particle size was minimized at a water-salt ratio of 2:1. In the temperature range of 220 to 350℃, Ag nanoparticles were successfully synthesized, the particle size (from 26 to 17 nm) and crystallite size (from 12 to 7 nm) both have a tendency to decrease with decreasing temperature, except that smaller and unusually larger silver particles appeared at the same time below 225℃ comparing to the product at higher temperatures. And the conversion of Ag^+ to Ag increased with increasing temperature below 300℃ (above 300℃: 99%). It was not feasible to prepare regular-shape nano-Ag from silver nitrate solution in subcritical conditions. The experiments on the treatment of Ag_2O powder in batch reactor demonstrated that in the continuous hydrothermal synthesis of nano-Ag, it may not be present as an intermediate product.

4.2 Prospect

Examining the results of experiments with different variables in an integrated way, it is possible that for the preparation of AgNPs, 350℃ is not low enough for exhibiting the effect of residence time on particle size and conversion, so time dependence below 300℃ (where the conversion begins to decrease) or a wider time frame requires further investigation. The variation of particle size with flow rate ratios implies that the size of AgNPs can be adjusted directionally. At lower subcritical temperatures, it is possible to

synthesize particles with sizes similar to those under supercritical conditions (15-30 nm), which is conducive to saving energy and easing the requirements for preparation equipment; And considering the abnormal grain growth and low conversion rate at temperatures lower than 225°C, the applicability of the corresponding products is low, but the tendency of particle size to decrease with temperature(235~350°C) can provide more options depending on the application requirements. Considering that the conditions under which Ag_2O is converted to Ag are likely to be different according to different Ag_2O states, perhaps Ag_2O colloidal precipitates will behave differently under supercritical or subcritical conditions than powdered products. The mechanism of continuous hydrothermal synthesis of AgNPs from silver salt without reducing agent requires further investigation in the future.

Reference

[1] Penghui Nie, et al. Synthesis, applications, toxicity and toxicity mechanisms of silver nanoparticles: A review. *Ecotoxicology and Environmental Safety*, **253**, 114636(2023).

[2] Shuhong Sun, et al. Progress in preparation and application of nanosilver. *Hans Journal of Nanotechnology*, **8** (2), 9-16(2018).

[3] A. M. Ealias, et al. A review on the classification, characterisation, synthesis of nanoparticles and their application. *Materials Science and Engineering* **263** (3), 032019(2017).

[4] Yaqoob, A.A, et al. Silver nanoparticles: various methods of synthesis, size affecting factors and their potential applications–a review. *Appl Nanosci* **10**, 1369–1378(2020).

[5] Sholikhah U, et al. Critical parameters of silver nanoparticles (AgNPs) synthesized by sodium borohydride reduction. *Res. J. Chem. Environ* **22** (Special Issue II), 179-183(2018).

[6] U.T. Khatoon, et al. Antibacterial and antifungal activity of silver nanospheres synthesized by tri-sodium citrate assisted chemical approach. *Vacuum* **146**, 259-265 (2017).

[7] A. Rónavári, et al. Green silver and gold nanoparticles: biological synthesis approaches and potentials for biomedical applications. *Molecules*, **26** (4), 844(2021).

[8] Wagner W, et al. The IAPWS formulation 1995 for the thermodynamic properties of ordinary water substance for general and scientific use[J]. *Journal of physical and chemical reference data*, **31** (2), 387-535(2002).

[9] J. W. Johnson, et al. Critical phenomena in hydrothermal systems: state, thermodynamic, electrostatic, and transport properties of H_2O in the critical region. *American Journal of Science* **291**, 541–648(1991).

[10] Toshihiko Arita, et al. Synthesis of iron nanoparticle: Challenge to determine the limit of hydrogen reduction in supercritical water. *The Journal of Supercritical Fluids*, **57** (2), 183-189(2011).

[11] Lamer, V. K., et al. Theory, production and mechanism of formation of monodispersed hydrosols. *J. Am. Chem. Soc*. **72**, 4847–4854(1950)

[12] M.N. Nichick, et al. *Polyhedron*, **28**, 3138-3142(2009).

[13] J.-Y. Lee, et al. *Polymer*, **47**, 7970-7979(2006).

[14] Y.Y. Xu, et al. *Analytica Chimica Acta*, **561**, 48-54(2006).

[15] Siyam M. Ansar, et al. Impact of gold nanoparticle stabilizing ligands on the

colloidal catalytic reduction of 4-nitrophenol. *ACS Catalysis*, **6** (8), 5553–5560(2016).

[16] T.S. Ahmadi, et al. Shape-controlled synthesis of colloidal platinum nanoparticles. *Science*, **272**, 1924-1926(1996).

[17] T.C. Deivaraj, et al. Solvent-induced shape evolution of PVP protected spherical silver nanoparticles into triangular nanoplates and nanorods. *J. Colloid Interface Sci.*, **289**, 402-409(2005).

[18] S. Kapoor. Preparation, characterization, and surface modification of silver particles. *Langmuir*, **14**, 1021-1025(1998).

[19] Libor Kvítek, et al. Effect of surfactants and polymers on stability and antibacterial activity of silver nanoparticles (NPs). *The Journal of Physical Chemistry*, **112** (15), 5825-5834(2008).

[20] T. Arita, et al. Synthesis of iron nanoparticle: challenge to determine the limit of hydrogen reduction in supercritical water. *The Journal of Supercritical Fluids*, **57** (2), 183-189(2011).

[21] S. Kubota, et al. Continuous supercritical hydrothermal synthesis of dispersible zero-valent copper nanoparticles for ink applications in printed electronic. *The Journal of Supercritical Fluids*, **86**, 33-40(2014).

[22] Kai Li, et al. Preparing silver nanoparticles in supercritical water. *Materials Letters*, **63** (3-4), 437-440(2009).

[23] Jia-Yaw Chang, et al. Silver nanoparticles spontaneous organize into nanowires and nanobanners in supercritical water. *Chemical Physics Letters*, **379**, 261–267 (2003).

[24] Junichi Otsu, et al. New approaches to the preparation of metal or metal oxide particles on the surface of porous materials using supercritical water: Development of supercritical water impregnation method. *The Journal of Supercritical Fluids*, **33** (1), 61-67(2005).

[25] G. Aksomaityte, et al. The production and formulation of silver nanoparticles using continuous hydrothermal synthesis. *Chemical Engineering Science*, **85**, 2-10(2013).

[26] W. E. Garner, et al. The thermal decomposition of silver oxide. *Trans. Faraday Soc.*, **50**, 254-260(1954).

[27] Tobisawa S. Magnetochemical investigation on thermal decomposition of silver Oxide. *Bulletin of the Chemical Society of Japan*, **32** (11), 1173-1180(1959).

[28] Nakamori Issei, et al. The thermal decomposition and reduction of silver(I) oxide. *Bulletin of the Chemical Society of Japan*, **47** (8), 1827-1832(1974).

[29] Lange's Handbook of Chemistry, Sixteenth Edition.

[30] Geoffrey I. N. Waterhouse, et al. The thermal decomposition of silver (I, III) oxide: A combined XRD, FT-IR and Raman spectroscopic study. *Physical Chemistry Chemical Physics*, **3** (17), 3838-3845(2001).

[31] Gimyeong Seong, et al. The reductive supercritical hydrothermal process, a novel synthesis method for cobalt nanoparticles: synthesis and investigation on the reaction mechanism. *Dalton Transactions*, **43**, 10778-10786(2014).

[32] Minsoo Kim, et al. Hydrothermal synthesis of metal nanoparticles using glycerol as a reducing agent. *The Journal of Supercritical Fluids*, **90**, 53-59(2014).

[33] Edward Lester, et al. Reaction engineering: The supercritical water hydrothermal synthesis of nano-particles. *The Journal of Supercritical Fluids*. **37**, 209-214(2006).

[34] Lu Zhou, et al. Size-controlled synthesis of copper nanoparticles in supercritical water. *Chemical Engineering Research and Design*. **98**, 36-43(2015).

[35] Sue, K., et al. Continuous hydrothermal synthesis of Fe_2O_3 nanoparticles using a central collision-type micromixer for rapid and homogeneous nucleation at 673 K and 30 MPa. *Ind. Eng. Chem. Res.*, **49** (18), 8841–8846(2010).

[36] Ed Lester, et al. Controlled continuous hydrothermal synthesis of cobalt oxide (Co_3O_4) nanoparticles. *Progress in Crystal Growth and Characterization of Materials*. **58** (1), 3-13(2012).

[37] F. Masoodiyeh, et al. Modeling zirconia nanoparticles prepared by supercritical water hydrothermal synthesis using population balance equation. *Powder Technology*. **317**, 264-274(2017).

[38] Lu Liu, at al. Supercritical hydrothermal synthesis of nano-ZrO_2: Influence of technological parameters and mechanism. *Journal of Alloys and Compounds*. **898**, 162878(2022).

[39] P. Cotterill, et al. *Recrystallization and Grain Growth in Metals* (1976).

[40] Yanling Liu, at al. Solvent annealing for high quality $MA_3Bi_2I_9$ perovskite thin films and solar cells. *Material Sciences*. **10** (1), 31-39(2020).

Acknowledgments

This thesis summarizes the results of my research over the past two years as a Master's student, and I would like to express my most heartfelt gratitude to those who have supported, encouraged and helped me in this process.

First of all, I would like to thank my supervisor, Associate Professor Akizuki-Sensei, for his patience and enthusiasm in giving me helpful advice and suggestions throughout my research process; In addition, Akizuki-Sensei's easy-going and friendly manner towards us has also greatly eased the pressure of my life and studies in the daily life.

And then I'd like to thank Professor Oshima-Sensei for his care and concern for each student and his ideals and passion for academic research, which touched me very much, as well as for his sincere advice on my research topic.

Matsushima-Sensei, my co-research advisor, was very kind and reassuring in giving me advice and support during the discussions, and I am very grateful for that.

Yajima-Sensei of the X-ray Measurement Room, Hamane-Sensei of the Electron Microscope Room and Ishii-Sensei of the Chemical Analysis Laboratory at the Institute for Solid State Physics, provided much guidance on TEM, XRD, and ICP-AMS measurement methods, respectively.

And appreciation to all the members in Oshima and Akizuki lab for giving me an enriched and enjoying school life. Thanks Wang Yongxu-San, a master's degree graduate, PhD student Wang Yiqi-San, and PhD student Li Fei-San, for guiding me in the experimental operation. I would like to express my special thanks to my classmate Xu-Kun for his help during the long experimental hours, and we had a lot of valuable discussions and experience sharing due to the proximity of the research topics.

Last but not least, I would like to thank my old friends who work in my hometown or study in other countries. Although I cannot meet them in person, they gave me a lot of spiritual comfort and support when I was in trouble and emotionally depressed.

Li Yanchen